List of changes applied to the manuscript

"Calibration of key temperature-dependent ocean microbial processes in the cGENIE.muffin (v0.9.123) Earth system model" by K.A.Crichton et al. for GMD.

We have:

Added the model version to the title of the manuscript

Added a new temperature-dependent DOM cycling option for cGENIE, and showed its impact on our main results, to address the comments from reviewer 1

Added a clarification on ocean circulation, with a caveat that we do not test any "extreme" warming scenarios in this paper. We have also adjusted the conclusion to clarify that we find temperature-dependent POM has offset (to a large) extent stratification induced nutrient limitation since the pre-industrial period (rather than stating it as a general pattern for warming).

Adjusted the equations to ensure that all have unique parameter identifiers.

Renamed the model configurations so they are more intuitive. CB becomes STND, CBRU becomes TDEP.

Provided more information on the statistical analysis, and provided the values for the fit to data for the main simulations in the text (as table 4).

We have improved all the figures, ensuring text is not too small to be legible.

We have addressed all the individual comments from the reviewers.

We have made general improvements to the text.

Response to reviewers, “Calibration of key temperature-dependent ocean microbial processes in the cGENIE.muffin Earth system model”

Response to reviewer 1

“Figure 2 highlights a key opportunity that has been overlooked in this study, which is that the fractional assignment of export to the DOM pool could easily be made temperature-dependent, and that would implicitly represent temperature-dependent fast recycling processes in the upper ocean. The authors should discuss why this parameter was not included in their calibration.”
We have added the option to the model of a temperature-dependence to both the production and remineralization of DOM, and assess the consequences of these new processes in the analysis of marine carbon cycling response to historical warming in the revised paper.
As described in a new and extensive subsection in the Discussion (5.2), adding temperature-dependence to the decay of DOM is relatively straight-forward as to a first order, one can start by assuming this takes place analogously to the decay of POM. Hence we adopt the same calibrated activation energy, but re-tune the scaling rate constant, as described in section 5.2.
The production of DOM is more problematic as available empirical equations such of Dunne et al. [2005], requires knowledge of either primary production (integrated across the mixed layer), or Chl*a*, neither of which is explicitly calculated in the standard (non ecosystem) configuration of cGENIE. (The standard configuration of the ocean circulation model also does not calculate a mixed layer depth.) We hence extracted just the temperature sensitivity from the regression model of Dunne et al. [2005] and apply this to the partitioning of POM vs. DOM in the model. And then tune this second parameterization.
While we find that the introduction of temperature-dependent processes in DOM cycling has a much lesser impact on global export than do temperature-dependent processes directly affecting POM, we agree with the reviewer that this makes for a more complete and rounded model development.

“Schmittner et al. 2008, GBC doi:10.1029/2007GB002953 Introduced a temperature dependent remineralization parameterization to the UVic ESCM…”
We have added Kvale et al 2015 and Kvale et al 2019 to those papers discussed in the introduction. And added Loptien and Dietze 2019 and Kvale et al 2019 to the discussion noting that circulation state is important for nutrient and carbon distributions.

“P6, Equation 5: Please either rename A or make it clear on this page that the value is different than the A in Equation 4.”
We have been through all the equations and terms in the entire manuscript, including the equations associated with the new DOM parameterizations, and ensure unique symbol choices for all parameters. (Capital ‘A’ we reserve for fractional sea-ice area only now and indeed, further clarify this by adding the subscript ‘ice’.)

“P7L89: Meyer et al. (2016) prescribed several e-folding depths, which approximates, but is not the same as, temperature dependence in export”
The reviewer is correct in that Meyer et al., (2016) prescribes different e-folding depths to parameterise the potential impacts of changing surface ecosystems in geological time on remineralisation, such as increasing organism size and complexity of trophic interations. Here we are

specifically referring to the export production scheme used that is the temperature-dependent scheme described by Monteiro et al., (2012). We have edited this sentence to better clarify and indeed now substituted the Monteiro et al. (2012) reference.

"P9L250: the North Pacific subsurface temperature profile is over-estimated in GENIE according to Fig 4, please correct this sentence"
Corrected in the text.

"P9L256: What are the lowest RMSE for CB and CBRU?"
We considered both the surface and full water column distributions to select the best-fit option for PO4: the (centred) RMSE for surface layer CB is 0.1700, CBRU is 0.1820; for whole ocean CB is 0.2208, CBRU is 0.2043 all in µmol/l. For O2 we use the whole ocean and depth layer 4 (283m to 411m), the (centred) RMSE depth layer 4 CB is 0.8145, CBRU is 0.8443; for whole ocean CB is 0.5476, CBRU is 0.5501 all in µmol/l. These values are represented in figure 5 and have been added to the main text for the STND (formerly CB) and TDEP (formerly CBRU) model and the new $TDEP_{+TDOM}$ configuration as table 4.

"P9L268: My understanding is the models are also tuned to O2 (from P9L253-256)"
Yes, this is correct. Added to the sentence in parentheses for clarity.

"P12L375: what is the Eastern Tropical North Pacific?"
This is a typo and should read "Eastern Tropical Pacific" – now corrected in the text.

"P13L380-381: DOM cycling is also changed"
We now explicitly address and discuss (in Section 5.2) how the DOM cycle is impacted by historical temperature rise, including now also accounting for temperature-dependent processes in DOM cycling. We also add 2 additional figures to the Appendix A (Fig A1 and A2) summarising the cycling of DOM, both in the present-day state, and the response to historical warming (as an anomaly), for all the main permutations of temperature-dependent parameterisations. We have noted that DOM may also be affecting NPP in tropical waters in section 5.1.

"P13 Summary: Please see Kvale et al. 2019 BG /10.5194/bg-16-1019-2019"
Kvale et al 2019 use a transient cold to warm simulation, the warm climate with over 1200ppm atmospheric CO2 and state that in the warm climate more phosphate is stored in the deep ocean due to longer residence time of deep waters. This scenario is entirely different to that used here where the transient simulation follows CO2 trajectory from 1700 CE to the present, with a max ~400ppm. At very high CO2 (such as 1200ppm) the AMOC (Atlantic meridional overturning circulation) is likely very much reduced or collapsed and this greatly reduces the return of deeper waters to the surface compared to a the situation with a strong AMOC at 400ppm (such as the present day). We have added the following to the main text in the discussion of the model response to historical warming:

"We note that circulation states and upwelling/downwelling changes can also have an impact on the distribution of carbon, oxygen and nutrients between the surface and the deep (Kvale et al 2019, Loptien and Dietze 2019), and are also model-dependent. Circulation changes are small between the pre-industrial and the present-day, unlike in the simulations in Kvale et al (2019) where very high CO_2 (up to 1200ppm) and high surface temperature results in large circulation pattern changes; increased nutrient storage in the deep ocean is

due to longer residence time of deep ocean water in that study (see Chikamoto et al. 2008 for the effect of Atlantic Overturning Circulation shutdown in cGENIE). In our study we have found that the temperature dependent biological pump offsets some of the effects of physical ocean response to warming (in increase near-surface nutrient recycling, so offsetting to some extent the effect of increased ocean stratification that otherwise reduces surface nutrients in the STND simulation). However, this is not to suggest that a temperature-dependent biological pump could offset the effect of extreme changes in circulation, such as an AMOC shutdown, or for far more extreme warming scenarios than that applied here. We do not test such scenarios here."

"Table 2 can be cut at no detriment to the manuscript. 'CB' and 'CBRU' are defined too late in the manuscript and the naming includes an extra (confusing) reference to BIOGEM. I suggest omitting the Table and renaming the simulations to something more descriptive, like 'Temp' and 'NoTemp', since all models contain 'Remineralization' and 'Uptake'."

We have retained Table 2 because it is now expanded with an additional alternative model configuration, now that we are also addressing DOM-linked temperature-dependent processes. However, we have noted the lack of intuitiveness in the 'CB' and 'CBRU' naming and have replaced these throughout the manuscript with the more intuitive "STND" and "TDEP" references. We have also added these references to the relevant parts in Section 2 that describe the standard and temperature-dependent model formulations.

"Figure 1 can be cut at no detriment to the manuscript"

This figure lays out the basic functioning of the biological pump, and visually summarises the two components of temperature dependence (in both nutrient uptake and remineralisation), as well as the partitioning of organic matter into POM and DOM – we think it is a useful overview of the components discussed in the text.

"Figure 2 caption: is "mixed player plankton" supposed to read "mixed phytoplankton"? Please add a key to clarify what dashed/solid/thick/thin lines, and shading, represent. Why is burial shown if there are no sediments? Should "nutrients" be PO4 (only PO4 in this model)? Why are autotrophic respiration/heterotrophic respiration/ consumers shown if they are not included in the model?"

We have improved the caption to figure 2 based on these comments:

"Figure 2. Schematic of biological pump processes showing where cGENIEs export production operates. In the export production model, no mechanistic consideration of the effects of temperature within the mixed-layer (i.e. GPP vs NPP vs community production) can be considered, but heterotrophic respiration (as remineralisation) vs community production (as export production) can be considered, as well as nutrient recycling. In this study we apply temperature dependency to Organic Matter production and remineralisation that drives the biological carbon pump. We do not model burial in this version of cGENIE (but it is here for completeness). In this cGENIE configuration, the nutrient is phosphate. Dashed line indicates the cycling of nutrient (and re-supply due to circulation). Solid lines indicates the cycling of carbon."

"Figure 8. I see why the figure is normalized (the point made on P9L275), but normalization is misleading (small differences of low concentrations appear to be significant). The figure would be more informative presented without normalization, but the above point can still be made in the text."

Figure 8 is now plotted also as absolute differences, not only as normalised differences, but with the normalised difference plot retained as it is directly referenced in the text and shows that largest

proportional changes (where an anomaly alone would tend to reduce the significance of changes in ocean regions that started with low nutrient concentrations that actually see the largest proportional changes). Nutrients limitation is important in the gyres, so any increase in concentration there would likely have a large impact on primary production.

All other technical corrections suggested by reviewer 1 have been applied to the text.

Response to reviewer 2

"At Ea(1) of >54.5 kJ/mol POC export becomes lower compared to the non-temperature dependent model. This could be concerning given that a small variation of the Ea(1) value (0.5 kJ/mol) results in completely opposite patterns compared to the findings of the study, i.e., the temperature-dependent model simulates lower POC export than the non-temperature dependent model. The uncertainty related to this finding does not come across clearly and should be discussed. Also, it does not seem necessary for circles to be color-coded to reflect different rPOM in Figure 11."

We thank the reviewer for highlighting that this is not clear. Partly this may have been due to a missing minus sign in the exponent of Equation 5 which has now been corrected. The relationship in Figure 11 of the manuscript is not immediately obvious as temperature is effectively fixed in the calibration runs. The reviewer is correct in noting a larger activation energy (Ea1) results a greater sensitivity of remineralisation rates to temperature (Figure 1, bottom panel). However, at a constant temperature, the remineralisation rate decreases as Ea1 increases (Figure 1 here, top panel). In our calibration runs (Figure 11 in the manuscript), atmospheric CO_2 is restored to 278 ppm such that climate and SSTs are invariant, i.e., temperature is constant across the calibration runs. Therefore, the increased activation energies tested lead to a decrease in remineralisation rate globally. This leads to deeper remineralisation of organic matter which drives the decrease in export production (e.g., Kwon et al., 2009, Nature Geoscience), but is still related to a greater sensitivity to temperature changes (Figure 1). We have added a brief explanation of this to the text describing Figure 11 in the manuscript as well as added the plates in figure 1 (here) to figure 11 in the manuscript to clarify this point.

The main finding of the study is that warming results in a drop in POC export for STND (-2.9%), but a rather smaller change in POC export for TDEP (at -0.3% for the best-fit setting). Even with Ea(1) at >55kJ/mol this pattern still holds because POC export is stimulated on warming in TDEP due to the increased nutrient recycling, now that remineralisation is temperature-dependent. Figure 11a shows only the global mean POC export at a fixed temperature, not how that export changes on warming. For higher Ea(1) that nutrient recycling increase on warming may be slightly lower, but certainly not such that the findings of the paper are inversed. Even with Ea(1) at 60 kJ/mol (Vmax =1, POC frac = 0.008), the drop in POC export for the historical period simulation is 0.43% (compared to the drop of 0.3% for TDEP best fit). The value of 54kJ/mol was selected as it shows a better fit to PO_4 and O_2 data (fig 5 main text) than other values.

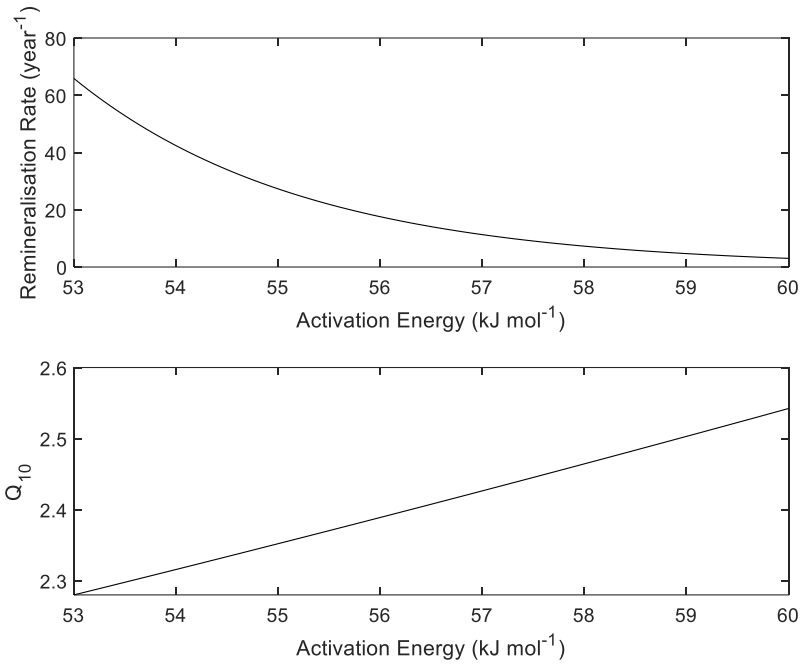

Figure 1. Top panel: The remineralisation rate calculated for with different activation energies for a constant temperature (273 K). Bottom panel: The Q_{10} of the remineralisation rate, i.e., the proportional change in the remineralisation rate for an increase in 10 K.

The colour coding on figure 11 reflects the colours used in figure 5, this has been added to the figure caption.

"In Introduction, in relation to "A deeper mean remineralization depth equates to a more "efficient" biological carbon pump" it would be good to calculate the remineralization depth as an additional measure of the biological pump efficiency from the model simulations. This could be helpful for cross-comparison with other modeling studies focused on the biological pump."

This is a useful suggestion from the reviewer. The key limitation of calculating a mean remineralisation depth here is that we are calibrating the model to observations such that the resulting values for STD and TDEP should be similar. We also note that the absolute mean remineralisation depth has been shown to be strongly dependent on ocean circulation (in particular the deep water formation in the North Atlantic) (Figure 6b in Kriest et al., 2020; Biogeosciences). As such, this is likely to be model dependent.

We note that a global value does not well represent the underlying characteristic identified in this study, where the remineralisation depth is entirely dependent on local conditions. In cold high latitudes the mean remineralisation depth is far deeper than in warm low latitudes. So, the resultant global mean will be somewhere in the middle. What then happens to the carbon in the deeper ocean is a function of ocean circulation and possible burial, so is heavily model-dependent. However, we have added this information to the main text in section 4.4 [627m for the standard model (formerly called CB) and 378m ± 236m for the T dependent model (formerly called CBRU)], and the

change in the global mean depth in section 5.1 for the historical period simulation [a shallowing of 16m for T-dependent model (formerly named CBRU)]. We have also added this information in section 5.2 for the additional DOM T-dependent model (the present-day is 399m ± 255m, and a shallowing of 16m since the year 1700).

"In Section 4.1 (line 244-251), it is discussed that cGENIE underestimates surface stratification and overestimates winter-time deep mixing due to an overly-strong AMOC in the physical circulation scheme of the model. The amount of phosphate returned to the surface is a function of deep mixing that increases organic matter production there, and this would not be modeled well if the model underestimated surface stratification. Uncertainties in the warming scenario results should be discussed."

We have added a paragraph in the discussion (in response to reviewer 1), that circulation plays a role in nutrient distribution as well, and that circulation is model dependent. We further note that cGENIEs reduction in export production (driven by an increase in stratification) through the pre-industrial to present warming agrees with the current state of the art in more complex models (CMIP5 models).

The winter time mixing overestimation was only for the North Pacific region (as indicated by the temperature profile there) not for the global ocean, and is not described as "due" to an overly-strong AMOC (which was only suggested as related to the N.Atlantic temperature profile). We do not do an extensive analysis of cGENIEs circulation in this study.

However, as we model a similar pattern of reduced export production in the standard model (due to increased stratification) that is shown in the mean of CMIP5 models, and we can fairly well model PO4 and O2 distributions in the present day we are reasonably confident that we have captured the large scale changes in circulation for the warming scenario. The warming scenario (the historical warming) compares the results from the different model configurations, which are all subject to the same changes in circulation that may be driven by that warming. Therefore we conclude that any differences in carbon cycle parameters are due to the temperature dependent biological processes, not circulation.

In Figure 2, the processes shown are not correct. Microbial (heterotrophic bacterial) respiration is also part of heterotrophic respiration (heterotrophic respiration = zooplankton respiration + bacterial respiration) and also occurs in the euphotic zone. The current schematic makes it look like microbial respiration is a separate process from heterotrophic respiration.

Reviewer 2 is correct. This separation between surface food web (heterotrophic respiration) and sub surface processes (microbial respiration) comes from the way they are often treated in models. Here surface food webs are modelled as being separate from sub surface processes like remineralisation, whereas actually this is not strictly the case in fact. The figure has been changed so that microbial respiration also reads "heterotrophic respiration". The aim of the figure is to demonstrate where cGENIEs export production model "sits" and hopefully makes the comparison to other models' treatments of the biological pump more straight-forward.

"In Figure 13, Please consider putting a global uniform value for POC transport efficiency in CB next to the CBRU plot, instead of presenting the stand-alone CB plot."

This value has been added to the caption for CB, but we keep the figure to really emphasise that including the temperature dependence makes a large difference to ocean carbon cycling.

"In all Figures, increase font size for better legibility as figure quality is currently poor; and use constant symbols in vertical profile figures for data, CB, and CBRU comparison."
Figure quality and legibility has been improved in the revised version for all figures.

All other technical comments from reviewer 2 have been included in the revised version.

Editor comment response

The title has been changed to include the model name and version:

Calibration of key temperature-dependent ocean microbial processes in the cGENIE.muffin (v0.9.13) Earth system model

We thank all reviewers for their comments.

K.A.Crichton on behalf of all authors.

Calibration of ~~key~~ temperature-dependent ocean microbial processes in the cGENIE.muffin (v0.9.12~~2~~3) Earth system model

Katherine A. Crichton[1*], Jamie D. Wilson[2], Andy Ridgwell[3], Paul N. Pearson[1].

[1] School of Earth and Ocean Sciences, Cardiff University, UK
[2] BRIDGE, School of Geographical Sciences, University of Bristol, Bristol, UK
[3] Department of Earth and Planetary Sciences, University of California, Riverside, CA 92521, USA
* now at School of Geography, University of Exeter, EX4 4RJ, UK

Correspondence to: Katherine A. Crichton (k.a.crichton@exeter.ac.uk)

Abstract. Temperature is a master parameter in the marine carbon cycle, exerting a critical control on the rate of biological transformation of a variety of solid and dissolved reactants and substrates. Although in the construction of numerical models of marine carbon cycling, temperature has been long-recognised as a key parameter in the production and export of organic matter at the ocean surface, ~~it is much less commonly taken into account~~its role in the ocean interior is much less frequently accounted for. There, bacteria (primarily) transform sinking particulate organic matter (POM) into its dissolved constituents and ~~thereby~~ consume dissolved oxygen (and/or other electron acceptors such as sulphate). The ~~and release~~ nutrients and carbon thereby released then become~~, which are then~~ available for transport back to the surface, influencing biological productivity and atmospheric pCO_2, respectively. Given the substantial changes in ocean temperature occurring in the past, as well as in light of current anthropogenic warming, appropriately accounting for the role of temperature in marine carbon cycling may be critical to correctly projecting changes in ocean deoxygenation as well as the strength of feedbacks on atmospheric pCO_2.

Here we ~~present~~ extend and calibrate ~~a more complete~~a temperature-dependent representation of marine carbon cycling in the cGENIE.muffin Earth system model, intended for both past and future climate applications. In this, we combine a temperature-dependent remineralisation scheme for sinking organic matter with a biological export production scheme that also includes a dependence on ambient seawater temperature~~temperature-dependent limitation on nutrient uptake in surface waters (and hence on phytoplankton growth)~~. Via a parameter ensemble, we jointly calibrate the two parameterisations by statistically contrasting model projected fields of nutrients, oxygen, and the stable carbon isotopic signature ($\delta^{13}C$) of dissolved inorganic carbon in the ocean, with modern observations. We additionally explore the role of temperature in the creation and recycling of dissolved organic matter (DOM) and hence its impact on global carbon cycle dynamics.

We find that for the present-day, the temperature-dependent version shows as-good-as or better fit to data than the existing tuned non-temperature-dependent version of the cGENIE.muffin. The main impact of ~~adding~~ accounting for temperature-dependent remineralisation of POM is in driving higher rates of remineralisation in warmer waters, in turn driving ~~and hence~~ a more rapid return of nutrients to the surface and thereby, ~~—~~ stimulating organic matter production. As a result, more ~~organic matter~~POM is exported below 80m but on average reaches shallower depths in mid and low latitude warmer waters, as compared to the standard

Formatted: Font: Italic
Formatted: Subscript
Formatted: Indent: First line: 1.27 cm

model. Conversely, at higher latitudes, colder water temperature reduces the rate of nutrient resupply to the surface and POM reaches greater depth on average as a result of slower ~~in situ~~sub-surface rates of remineralisation ~~and POM reaches greater depth on average~~. Further adding temperature-dependent DOM processes changes this overall picture only a little, with a slight weakening of export production at higher latitudes.

~~We~~ As an illustrati~~veon~~ application of the new model configuration and calibration, we take the example of historical warming ~~also~~and briefly assess the implications for global carbon cycling of accounting for a more complete set of temperature-dependent processes in the ocean~~, for which of including a more complete set of temperature dependent parameterisations by analysing a series of historical transient experiments~~under historical warming. We find that between ~~the~~ pre-industrial (ca. 1700) and ~~the~~ present ~~day~~(year 2010), in response to a simulated air temperature increase of 0.9°C and an associated projected mean ocean warming of 0.12°C (0.6°C in surface waters and 0.02°C in deep waters), a reduction in particulate organic carbon (POC) export at 80m of just 0.3% occurs (or 0.7%~~xxx~~ including a temperature-dependent DOM response). However, due to this increased recycling nearer the surface, the efficiency of the transfer of carbon away from the surface (at 80m) to the deep ocean (at 1040m) is reduced by 5%. In contrast, with no assumed temperature-dependent ~~biological~~ processes impacting~~ any of the~~ production or remineralis~~z~~ation of either POM or DOM, global POC export at 80m falls by 2.9% between the pre-industrial and present day as a consequence of ocean stratification and reduced nutrient resupply to the surface~~. This suggests that increased nutrient recycling in warmer conditions offsets some of the stratification-induced surface nutrient limitation in a warmer~~ rapidly warming world, and ~~with~~that less carbon (and nutrients) then reaches ~~reaching the inner and deep ocean~~ocean interior~~. This extension to the cGENIE.muffin Earth system model provides it with additional capabilities in addressing marine carbon cycling in warmer past and future worlds.~~ by 5% between 80 and 1040m depth~~. Between 1700 and 2010 CE, we simulate a reduction of over 5% in the proportion of carbon exported at 80m that reaches 1040m depth~~. Our analysis suggests that increased temperature-dependent nutrient recycling in the upper ocean has offset much of stratification-induced restriction in its physical transport.

Formatted: Font color: Auto

Commented [m1]: I sort of alluded to this in the new sentence at the end of the (now split) 1st paragraph.

1 Introduction

The cycle of carbon through the ocean is dominated by the production, destruction, and transformation of both dissolved and particulate organic matter (DOM and POM, respectively) (Legendre et al., 2015; Heinze et al., 2015). The 'biological carbon pump' (Fig. 1) ~~is a principal mechanism~~is central in this ~~–~~, ~~operating by removing~~acting through phytoplankton growth to remove carbon (and nutrients) from the surface and mixed layer waters, ~~by phytoplankton photosynthesis~~ and subsequently transferring it to the deep, principally ~~by~~ via the sinking of POM~~organic matter~~ (see: Hülse et al., 2017 for a review) and to a lesser extent, via the subduction of DOM. Export of POM out of the near-surface euphotic zone is ~~affected~~ principally controlled by photosynthesis rates (primary production) together with~~, but is also affected by~~ zooplankton grazing, respiration, and other food web processes (Steinberg and Landry, 2017; Mari et al., 2017). Of this export, only a fraction ultimately reaches the deep ocean ~~through~~ as the initial export flux is filtered through a series of further processes and transformations involving feeding and remineralisation by microbes and other biota, and further modulated by sinking speeds and composition of the sinking matter itself (Bach et al., 2016; Rosengard et

al., 2015; Turner, 2015). At the ocean floor, organic matter undergoes further microbial degradation and transformation before the residual is buried~~eventually forming~~ in accumulating marine sediments. Removing carbon from surface waters and storing it for centuries (intermediate depths), millennia (deep ocean), or multi-millennia (sediments) ex~~p~~erts an important control~~s~~ on atmospheric pCO_2 ~~levels~~ , which would otherwise be ~~much higher (by ~~some 150ppm to 200ppm~~)~~ higher than present in the absence of ~~this~~any biological activity in the ocean (Parekh et al 2005, Sarmiento and Gruber, 2006). Ocean circulation generally acts against the biological pump, geochemically homogenising ~~heterogeneity in~~ the ocean interior and returning carbon (and nutrients) back to the surface. Surface-to-deep geochemical gradients and storage of carbon in the ocean is hence a function of the rate of ocean ventilation in conjunction with the rate of biological export of carbon ~~export~~ from the surface and importantly, the ~~mean depth~~rate at which the organic matter is remineralised in the ocean interior.

To a first order, export of carbon out of the mixed layer in a ~~warmer~~ warming world will be reduced as a consequence of increased ocean stratification reducing nutrient re-supply to surface waters (Portner et al., 2014; Reusch and Boyd, 2013). ~~At the same time, higher water temperatures will increase the metabolic rates of photosynthesising and respiring organisms (Brown et al., 2004). Because respiration is much considerably more sensitive to temperature than photosynthesis, this may put further pressure on nutrient demand in surface waters affecting primary production and also, therefore, affecting the rate of carbon export (Boscolo-Galazzo et al 2018).~~ However, the export of carbon ~~and the 'strength' of the biological pump~~ is only one of the pertinent factors in marine carbon cycling. Also important is the 'transfer efficiency' of the biological pump – the fraction of exported carbon that reaches the inner ocean, or alternatively, the mean depth below the surface at which this carbon is remineralised, and dissolved inorganic carbon (DIC) returned to the ocean. A deeper mean remineralisation depth equates to a more transfer-~~'~~efficient~~'~~ biological carbon pump. The sub-surface processes that affect the biological carbon pump efficiency are also temperature-dependent (Bendtsen et al., 2015; Turner 2015; Boscolo-Galazzo et al 2018), complicating the net response of the biological carbon pump and carbon sequestration in the ocean interior to changes in global warming.

~~Until recently, few modelling studies considered sub-surface processes in the ocean carbon cycling response to temperature change (Kvale et al., 2019; Yamamoto et al., 2018; Cao and Zhang 2017; Laufkotter et al., 2016; Kvale et al., 2015; Segchneider and Bendtsen, 2013; Chikamoto et al 2012).~~ Not all ocean biogeochem~~e~~ical models and associated global carbon cycle studies~~Kvale et al., 2019; Yamamoto et al., 2018; Cao and Zhang 2017; Laufkotter et al., 2016; Kvale et al., 2015; Segchneider and Bendtsen, 2013; Chikamoto et al 2012~~ account for temperature controls on (and hence efficien~~cy~~t of) the biological carbon pump (some that do~~,~~ include: Kvale et al., 2019; Yamamoto et al., 2018; Cao and Zhang 2017; Laufkotter et al., 2016; Kvale et al., 2015; Segchneider and Bendtsen, 2013; Chikamoto et al. 2012; Moore et al. 2002). Hulse et al. (2017) presented an extensive review of how EMICs (Earth System Model of Intermediate Complexity) and box models treat ocean carbon cycle processes and summarised how inner ocean processes are less well constrained than surface processes in many models and how their treatment in models is much more variable. This is also the case for more complex ocean models, such as those participating in CMIP5 (Coupled Model Inter-comparison Project 5) and used to inform the recent IPCC assessment (Bopp et al.2013, Burd et al., 2016). ~~Making~~ However, temperature-dependency of inner ocean processes ~~temperature-dependent in models~~ has been found to have an important impact on

Commented [m2]: Unclear sentence.

Commented [CK3R2]: changed

nutrient distribution and, therefore, on primary production (Tauscher and Oschlies, 2011) as well as biological pump efficiency (Laufkotter et al., 2017), arguing for the necessity of their inclusion in models.

In a warmer world, hAll things being equal, higher ocean temperatures should drive a greater fraction of remineralisation to occur in the upper water column, facilitating increased carbon and nutrient return to the ocean surface. Higher surface temperature will also increase the ability of phytoplankton to take up and assimilate the resulting increased nutrient availability and hence re-export POM, although grazing pressure would also increase. However, higher temperatures also lower the solubility of CO_2 solubilityat the surface and hence loss to the atmospherewill also increase carbon loss at the surface due to lower CO_2 solubility, while at the same time promoting biological carbon uptake. Furthermore, for a geologically rapid and transient warming at the surface such as is currently occurring, increased ocean stratification and hence reduced physical transport of carbon and nutrients back to the surface, will occur. The multiple conflicting influences of temperature mean that even the net sign of the feedback between greenhouse warming and ocean carbon cycling is, at the very least, unclear uncertain (Yamamoto et al 2018). (How carbon fixed at the surface is recycleding via partitioning into DOM rather than exported as POM, and the rate at which DOM itself is recycled back into dissolved carbon and nutrients as temperatures rise, then adds another complicating layer of temperature response and feedback.)

To help tease apart the varying influences of temperatures on marine carbon cycling and atmospheric CO_2, we present and calibrate a temperature-dependent representation of the biological pump in the current 'muffin' release of the cGENIE EMIC (Earth system Model of Intermediate Complexity) (Cao et al. 2009) (and see statement on 'Code Availability'). Our calibrated configuration is intended for use in global biogeochemical cycling studies that require a fuller consideration of the role of temperature both in the geological past and the future. For completeness, we additionally develop and test a pair ofr parameterisszations for temperature-dependency in the production and decay of DOM.

2 The cGENIE.muffin Earth system model framework (STND)

The basic framework of the cGENIE EMIC consists of a 3D frictional-geostrophic approximation ocean circulation model (Edwards and Marsh, 2005), coupled to a 2D dynamic-thermodynamic sea-ice model (Marsh et al., 2011). As per previous calibrations of ocean biogeochemical cycles (e.g. Ridgwell et al., 2007), we employ the ocean circulation and sea-ice model on a 36 x 36 equal area grid (10 degrees of longitude and uniform in the sine of latitude), and couple these with a 2D energy-moisture-balance atmosphere model (EMBM) (Marsh et al., 2011) (an alternative to this – a 3D atmospheric general circulation model (Holden et al., 2016) also exists, but is not employed in this study). We For traceability, we employ a commonly-used physical configuration with 16 vertical levels in the ocean and a present-day bathymetry following Cao et al. (2009). All and retain all physics parameter valuess and boundary conditions controlling the climate system follow Cao et al. (2009). The representation of the ocean carbon and other biogeochemical cycles together with ocean-atmosphere gas exchange, unless otherwise noted, also follow Cao et al. (2009), and are summarised in more detail below. The various temperature-dependent parameterisations that we substitute for the equivalent non temperature-dependent processes in Cao et al. (2009) are described in full in this paper.

Formatted: Subscript

It ~~has been suggested that~~is likely that both increased grazing pressure ~~(respiration process)~~ by zooplankton, and primary production by phytoplankton ~~(photosynthesis process),~~ will have an impact on export production in a warmer world (Paul et al., 2015; Turner, 2015). However, in the simplified biologically induced export flux (Maier-Reimer, 1993) scheme (Fig. 2) that we apply in cGENIE, we cannot explicitly consider the impact of increased grazing pressure in the surface waters. Regardless~~ather~~, we are interested in the wider question of the interaction of (any) temperature-dependent community production (as export production), with temperature-dependent microbial remineralisation in the ocean interior, and its impact on the global ocean carbon cycle. We hence ~~apply~~ represent only the direct effect of temperature on large scale metabolic processes (plankton photosynthesis (growth) and microbial respiration). Other factors such as involving particle size distributions, particle density (Cram et al., 2018) and 'ballasting' (e.g. Wilson et al., 2012), and sinking speed (determined by particle characteristics) (McDonnell et al., 2015), are generally determined within the food web and may be considered ~~in the context of the gross role of temperature in global carbon cycling.~~ to be of secondary ~~impacts of temperature dependence as a controller on community structure~~importance in the context of the gross role of temperature in global carbon cycling. ~~In past climates some of these community structures may have been significantly different. We also do not alter the production or cycling of dissolved organic carbon (DOC) compared to the standard model (Ridgwell et al 2007).~~ Recently, Boyd et al. (2019) defined additional particle pumps in the ocean, involving eddy-subduction, diel vertical migration, mesopelagic migration and seasonal lipid pumps. ~~We consider that IiTIncluding t~~hese processes ~~is we consider also to be~~are also outside the scope of this study, particularly ~~where here we focus on the large-scale effect of temperature on metabolism in the ocean biological carbon pump~~in the absence of ~~much higher~~a sufficiently high resolution ~~in the~~ ocean circulation model component, the absence of (fully coupled GCM) ocean-atmosphere dynamics and inter-annual variability, and without an explicit ecosystem including multiple trophic layers and explicit zooplankton behaviours.

2.1 Standard, non-temperature-dependent model formulation (STND)

In the original version of the biological uptake scheme~~, 'BIOGEM'~~ (Ridgwell et al., 2007)~~.~~, nutrients are taken out of the surface ocean layer according to several factors including light incidence, ice fraction, nutrient uptake limitation (Michaelis-Menten type), and a prescribed maximum uptake rate (Eq. 1). In this, Γ, the net nutrient uptake (mol PO_4 kg^{-1} yr^{-1}) and hence net primary production in the surface ocean layer of the model, is described as:

$$\Gamma = u_0^{PO_4} . \frac{PO_4}{PO_4 + K^{PO_4}} . (1 - A_{ice}~~4~~) . \frac{I}{I_0} \quad (1)$$

w~~W~~here:

$u_0^{PO_4}$	maximum uptake rate (mol kg^{-1} yr^{-1})
$\frac{PO_4}{PO_4 + K^{PO_4}}$	nutrient limitation term
PO_4	local nutrient concentration (mol kg^{-1})
K^{PO_4}	Michaelis Menten half saturation value (mol kg^{-1})

Formatted: Font: Italic
Formatted: Subscript
Formatted: Superscript
Formatted: Superscript

$1 - A_{ice}$ ~~4~~ ice free fraction of sea surface (A_{ice} being the ice-covered fraction of a grid cell)

$\frac{I}{I_0}$ light limitation (based on incidence angle) term

Here, ~~the~~ a maximum uptake rate, (maximum rate of conversion of dissolved PO_4, phosphate, into organic matter by phytoplankton) is prescribed, ~~has~~ and is assigned a calibrated value of 9.0 x10^{-6} mol kg^{-1} yr^{-1} (Cao et al., 2009), while the calibrated Michaelis Menten half saturation value is 9.0 ×10^{-7} mol kg^{-1} (Cao et al., 2009).

Nutrient uptake is instantaneously converted into organic matter export ~~(~~, both particulate organic matter (POM) and a fraction as dissolved organic matter (DOM), in a ratio of 1:2 following Najjar et al. ~~[~~(2007)~~]~~, and this represents community production (see Fig. 2). This production encompasses the entire surface food web, including the action of primary producers (phytoplankton) and the effect of consumers (e.g. grazers). In this export production model, ~~increases in nutrient uptake are directly transferred to increased production of organic matter that sinks out of the surface layer (at 80m depth). In this single (PO_4) nutrient scheme,~~ dissolved inorganic carbon (DIC) is taken out of solution in the surface layer at a molar ratio of 106:1 to PO_4 and O_2 at a ratio of - 138:1 with PO_4 (Redfield et al., 1963). POM is partitioned into two fractions, which conceptually are: labile (fraction 1, 'POM1'), and recalcitrant POM (fraction 2, 'POM2') (Ridgwell et al., 2007). POM sinks vertically out of the surface layer and settles with a given velocity (here: 125 m day^{-1}). POM is remineralised throughout the water column using a prescribed remineralisation 'curve' reflecting the decay of POM as it sinks, first using dissolved oxygen and then sulphate. The prescribed remineralisation 'curve' of relative sinking flux vs. depth (e.g. see: Hülse et al., 2017) is always adhered to (Eq. 2a for POM1, Eq. 2b for POM2). In the sinking curve, the relative flux at each layer (z) is calculated according to an exponential decay function (Ridgwell et al., 2007).

$$F_z^{POM1} = F_{z=h_e}^{POM1} \cdot \left((1 - r^{POM}) + r^{POM} . exp\left(\frac{z_{h_e} - z}{l^{POM1}}\right)\right) \quad (2a)$$

$$F_z^{POM2} = F_{z=h_e}^{POM2} \cdot \left((r^{POM}) + r^{POM} . exp\left(\frac{z_{h_e} - z}{l^{POM2}}\right)\right) \quad (2b)$$

w~~W~~here:

$F_{z=h_e}^{POM}$ POM exported out of the surface layer (at 80m)

l^{POM} length-scale (556m for POM1; 1x10^6m for POM2 – effectively infinite and hence no water column decay)

r^{POM} initial proportion of POM into fraction 2 (0.055)

Any POM not remineralised within the water column is instead remineralised at the ocean floor – a 'reflective' boundary condition assumption (see Hulse et al. (2017) for discussion). DOM is degraded with a lifetime of 0.5 years following Najjar et al. (~~[~~2007)~~]~~.~~,~~

2.2 Temperature- dependent processes (TDEP)

In ~~the~~ an alternative ~~temperature-dependent version~~ representation of biological export production in the model, a temperature-dependent growth rate limiter is applied to a characteristic time-scale of ambient nutrient depletion (Eq. 3). A similar scheme (but without the addition of temperature-dependent remineralisation in the ocean) has previously been applied by Meyer et al. (2016) for PO_4-only uptake, and for 2 nutrients (PO_4 and NO_3) by Monteiro et al. (2012). In this, net nutrient uptake (mol PO_4 kg^{-1} yr^{-1}) is:

$$\Gamma = V_{max} \cdot \frac{PO_4}{PO_4 + K^{PO_4}} \cdot (1 - A_{ice}\cancel{A}) \cdot \frac{I}{I_0} \cdot \gamma^T \cdot PO_4 \quad (3)$$

~~W~~where:

γ^T	temperature growth limitation term (see below)
V_{max}	maximum net depletion rate multiplier (yr^{-1})
PO_4	local PO_4 concentration (mol kg^{-1})
$\frac{PO_4}{PO_4 + K^{PO_4}}$	nutrient limitation term
K^{PO_4}	Michaelis Menten half saturation value (mol kg^{-1})
$1 - A_{ice}\cancel{A}$	~~———~~ice-free fraction of cell
$\frac{I}{I_0}$	light limitation (based on incidence angle) term

Temperature growth limitation is represented by the Arrhenius equation, where T is local temperature (Eq. 4).

$$\gamma^T = \cancel{A}ae^{(T/b)} \quad (4)$$

Th~~is is the~~e "Eppley curve", ~~is~~ commonly~~often~~ applied to model metabolic response to temperature change (Table 1). An improved fitted curve was proposed by Bissinger et al. (2008) (the LPD or Liverpool Plankton Database curve), with both being based on fitting the model to data from empirical studies. The largest difference between the Bissinger curve and the Eppley curve is the value of $a\cancel{A}$ (Eq. 4, Table 1). It makes little difference which curve we use because we calibrate V_{max} (Eq. 3) which is also a multiplier for the temperature growth limitation term (in Eq. 4). We use the original Eppley et al. (1972) values for $A\cancel{a}$ (0.59) and b (75.80), ~~(in Eq. 4)~~and as per Monteiro et al. (2012). Both the Eppley and Bissinger curves gives a Q_{10} value (where Q_{10} is the increase in the rate of the metabolic process with a 10°C increase in temperature) for nutrient uptake as 1.88 (Bissinger et al. 2008).

To calculate the remineralisation rate of POM (mol yr^{-1}), an Arrhenius-type equation is applied (as in John et al., 2014) (Eq. 5).

$$k(T) = \beta_{POMn}\cancel{A}e^{(-E_a/RT)} \quad (5)$$

~~W~~where:

E_a	Activation energy (J mol^{-1})

Formatted: Subscript
Formatted: Superscript
Formatted: Superscript
Formatted: Superscript

R gas constant (J K^{-1} mol^{-1})

T absolute temperature (K)

β_{POMn}~~A~~ rate constant for POM remineralisation (yr^{-1}) as T approaches infinity (for each POM fraction)

This rate is calculated ~~for~~ in each ocean layer (and model grid point) according to the local temperature~~, and applied to the local~~ POM flux, and for each of the two~~2~~ POM fraction~~s individually~~. For both fractions, sinking rate is assumed to be 125 m day^{-1} (Ridgwell, 2001), so for cGENIE's non-uniform ocean depths, the fractional loss of POM due to remineralisation in each layer (z) is as Eq. 6.

$$\Delta F_z^{POMn} = k(T)_z^{POMn} . \Delta t(z) \quad (6)$$

w~~W~~here n denotes POM fraction (either labile (1) or recalcitrant (2) - distinguished as these have different $k(T)$ values), $\Delta t(z)$ is the time that sinking particles on average spend in layer z.

~~(~~We will describe and evaluate the impact of processes accounting for the influence of temperature on both the production (ratioed to POM) and degradation of DOM, as part of the Discussion section.~~)~~

3 Model tuning methodology

In previous published applications of the cGENIE model, either a temperature dependence in calculating export (but not ocean interior mineralisation) (e.g. Meyer et al. 2016, Monteiro et al. 2012~~Meyer et al., 2016~~) OR a temperature dependence in remineralisation (but not biological productivity) (John et al., 2014) have been ~~explored~~ utilised in addressing varying paleo questions. ~~Or m~~More commonly, neither have been utilised (e.g. Ridgwell and Schmidt, 2010)~~, have been used~~. Here, we ~~now~~ explor~~eing~~e both temperature dependenc~~iesy~~e ~~in export as well as in nd remineralisation scheme~~ together (Table 2). Although~~-~~ in John et al.~~,~~ (2014)~~,~~ the temperature~~-~~dependent remineraliz~~s~~ation scheme was calibrated to approximate the global mean POM de~~l~~ay profile in~~of~~ the default ~~(i.e. Ridgwell et al., 2007)~~ model (i.e. Ridgwell et al., 2007)~~-~~ under pre-industrial boundary conditions, here we adopt a more formal re-tuning against observations of ~~and as a consequence, it is necessary to jointly re-tune~~ the ~~respective~~ primary scaling factors in each scheme.

We identify three primary parameters ~~needing~~ requiring joint re-tuning: 1, t~~T~~he maximum nutrient uptake rate V_{max} (Eq. 3) ~~important~~ that scales ~~for~~ export production. 2, t~~T~~he activation energy, $E_a(1)$ (Eq.5) (the minimum energy required for the transformation of organic carbon into inorganic carbon through respiration processes for the remineralisation of labile POC1, Particulate Organic Carbon type 1) where the labile POC1 dominates ~~that~~ the export~~ed~~ from the surface. ~~-~~3, t~~T~~he fraction of recalcitrant POC2 (denoted as *rPOM* Eq.2a and Eq.2b~~, note that in this paragraph values are described for carbon, but apply for nutrient as well~~) formed at the surface that ~~that plays a role in the down-column total POC flux and especially how much of the total POC~~ reaches the very deep ocean.

The V_{max} range was chosen by ~~testing the model~~running a series of test simulations (a 10k year spin up with pre-industrial boundary conditions followed by the historical transient simulation forced with CO_2 data to the present day) varying V_{max} while retaining the temperature-dependent remineralisation ~~version~~ scheme ~~used~~ adopted in John et al. (2014)~~.~~. From these results ~~and~~we selec~~ted~~ting a range of values for the multiplier V_{max} that gave a reasonable agreement with PO_4 and O_2 ~~concentrations~~distributions~~.~~; ~~at~~these V_{max} values are 4, 7 and 10. For the initial fraction of POC2, we took the John et al. (2014) ~~version~~value (with POC2 fraction of 0.008), and applied a ~~testing~~ range that encompassed ~~a range~~ 25% to ~~-~~400% around ~~this value~~ that value~~(×0.25, ×1.0, ×4.0)~~. For the $E_a(1)$ (Eq.5) setting, John et al. (2014) used a value of 55 kJ/mol, the m~~edian~~id of a range of 50 to 60 kJ/mol for labile POC ~~(range~~ identified in Arndt et al. ~~(~~2013~~))~~. We test~~use a lower and higher value of that range~~ a series of values for $E_a(1)$ within the range ~~, and a selection of values nearer the mean~~ (Table 3). Our ensemble hence consisted of 3 different choices for V_{max}, 3 different choices for initial fraction of POC2, and 5~~6~~ different choices for $E_a(1)$, for a total of 3×3×5 = 45 different parameter combinations and hence model ensemble member experiments. Values for the two rate constants, β_{POM}~~A~~ (Eq 5, for POC1 at 9×10^{11} yr^{-1}, for POC2 at 1×10^{14} yr^{-1}) that were calibrated for the modern ocean and the sinking speed of 125 m day^{-1} in John et al. (2014) are retained.

Each of the 45 experiments in the ensemble are spun-up for ten thousand years ~~with~~ under pre-industrial boundary conditions: ~~the~~ atmospheric pCO_2~~e~~ is ~~continually~~ restored to 280 ppm ~~CO_2~~ and with a $\delta^{13}CO_2$ isotopic value of -6.5 ‰ ~~$\delta^{13}CO_2$~~. To contrast the model ensemble members with observations, model-data comparison based on ~~the model~~a simulated pre-industrial steady-state creates a mis-match because global datasets are based on modern (i.e. the past few decades) oceanographic observations, where (especially shallow) distributions of nutrients and oxygen ~~may already~~ have already been impacted by historical warming. Therefore, ~~F~~following on from each respective spin-up, each model ensemble member is ~~hence~~ then forced from year 1700 to 2010 in a transient simulation with atmospheric composition conforming to the observed ~~(rising)~~ mean annual trend~~s~~ in CO_2 ~~and (falling) $\delta^{13}CO_2$. This is because global datasets are based on modern (i.e. the past few decades) oceanographic observations, where (especially shallow) distributions of nutrients and oxygen may already have been impacted by historical warming, so model-data comparison with the model pre-industrial steady-state is arguably inappropriate.~~ Direct atmospheric measurements and ice core data has shown that atmospheric $\delta^{13}CO_2$ has dropped with increasing CO_2 due to fossil fuel emissions (that have a characteristic low $\delta^{13}C$) known as the Suess effect (Keeling, 1979; Rubino et al., 2013). This affects ocean $\delta^{13}C$ in a non-uniform manner – ~~affecting~~ impacting (in general) nearer-surface waters more strongly due to ocean physics and circulation patterns. We hence additionally force atmospheric composition in the transient simulations with declining $\delta^{13}CO_2$ (Francey et al., 1999).

3.1 Model-data comparison method

For the model-data comparison, World Ocean Atlas 2009 (WOA 2009, Levitus et al. 2010) 5° gridded climatological data for phosphate (PO_4) and dissolved oxygen (O_2) was ~~rescaled~~ interpolated to a 10°x10° grid (with a simple linear upscaling), and then to the cGENIE model depth scale by averaging over the data depth points that most closely correspond to the cGENIE ocean model depth layer distribution. This depth rescaling produce~~d~~s a global mean depth-uncertainty of 2.2% (of the targeted cGENIE depth). ~~As a result T~~the depth rescaling result~~ed~~s in minor additional ~~small~~ uncertainties of ± 0.01µmols l^{-1} (at 1 standard deviation) for PO_4, and ± 0.02 µmols l^{-1} for dissolved O_2~~.~~ in addition to the error inherent in the gridded climatology product.~~–~~ For a direct

Formatted: Not Superscript/ Subscript
Formatted: Not Superscript/ Subscript
Formatted: Not Superscript/ Subscript
Formatted: Font: Italic
Formatted: Font: Italic, Subscript

comparison with the data. ~~The~~ cGENIE model output from year 2010 of the transient experiments was also ~~rescaled~~ interpolated to 10°×10°, and converted to units of µmols l^{-1} (from mol kg^{-1} using modelled water density) ~~for modelled O_2 and PO_4, for a direct comparison with the data~~. ~~In all cases~~L, ~~l~~atitudes higher than 80° were neglected due to higher uncertainties in both data and model outputs. For PO_4, we statistically compared the surface concentration, important for constraining nutrient uptake rates, ~~and~~ as well as the global ocean distribution, which strongly reflects remineralisation and hence the strength and efficiency of the biological pump (plus ocean circulation). For dissolved O_2, we statistically compared model and data ~~just~~ between 283m to 411m (cGENIE ocean level 4 centred at 346m) as an indication of the dissolved oxygen depletion caused by remineralisation near the bottom of the mixed layer and how well the model can represent this. ~~We also~~ As ~~for~~with phosphate, we additionally compared the model global ocean dissolved oxygen distribution with data. ~~Given~~ Finally, given that we are utilizing model-derived temperature distributions in the ocean to project nutrient and oxygen concentrations (plus $\delta^{13}C$ distributions) which we then contrast with the respective observed data, we ~~additionally re-grid~~interpolated temperature data (producing an uncertainty of ±0.1°C) in the same way as O_2 and PO_4 so as ~~to enable us~~ to elucidate biogeochemical biases arising from model-data temperature mismatch.

To evaluate the model skill, we compared model to data standard deviation (SD), calculated the centred root mean square (CRMSD) difference between model and data, and calculated model-data correlation, these parameters can then be presented on a Taylor plot. On this plot the general proximity of the model point to the data point indicates the goodness of fit, as well as a providing a visual comparison of how the changing parameters affect the model skill.

For assessing water column profiles, we defined a set of ocean regions as~~,~~ shown in Figure 3. These regions are similar to those used by Weber et al. (2016), but with some regions reduced in size or separated (Subtropical Pacific limited to South Pacific and North Indian Ocean added). This was done so that within each region, ocean water characteristics ~~are broadly similar~~ (including temperature, nutrients, oxygen, salinity) as well as particle fluxes ~~being similar~~ (as Weber et al. 2016) are broadly similar. We compare the model distribution of $\delta^{13}C$ of DIC with data from Schmittner et al. (2013) by grouping this data into regions (Fig. 3) and creating representative (mean with standard deviation) down-column profiles for $\delta^{13}C$ for visual comparison with model outputs in the matching region.

4 Model-data and model-model comparison

4.1 Tuning the temperature-dependent version – model vs. data

We first assess model skill in simulating the temperature distribution in the ocean, given its critical importance in the temperature-dependent calculations of metabolic processes (Fig. 4). We find a generally ~~good~~ reasonable model fit to ocean temperature data in mid and low latitude~~s~~ near-surface waters, and in capturing the first order patterns in benthic temperatures. At high latitudes, cGENIE shows larger differences as compared with observations~~,~~ due to deficiencies in modelled ocean circulation and/or the surface climate as simulated in the simple 2D EMBM. For instance, the temperature discrepancy throughout the water column in the North Atlantic may be due to an overly-strong AMOC (Atlantic Meridional Overturning Circulation) in the model that delivers

too high a volume of warmer surface waters to depth. For the North Pacific, the model ~~underestimation~~ overestimation of ~~surface and~~ near-surface temperatures by cGENIE likely reflects insufficient surface stratification~~; and~~ too-deep downwards ~~winter-time~~ mixing transporting too-warm surface waters to mid depths ~~of the upper water column~~in this location.

The ensemble simulation results (year 2010 of the transient experiments) for the ocean geochemistry are shown in Fig. 5 on Taylor diagrams for their fit to observed distributions of dissolved PO_4 and O_2 in the ocean. Points in Fig. 5 are shaded according to the $E_a(1)$ (Eq.5) value, which has the strongest control on PO_4 and O_2 distribution of the three variables. The overall best-fit to the data for the final ~~CBRU~~TDEP setting was selected as V_{max} = 10, $E_a(1)$ = 54 kJ mol^{-1}, initial fraction POC2 = 0.008, where the best-fit is determined as the setting with the combined overall lowest CRMSD~~E~~ for the PO_4 and O_2 distributions. The CRMSD for each variable is shown on Fig. 5 as the radial distance from the data point (the radial axis coloured green). In general the parameter value combinations with lowest CRMSD values corresponds with highest correlations in the model fit to data (Fig 5). The statistics for the STND and best fit TDEP are listed in Table 4.

~~Surface nutrients are important in constraining export production. Fig. 6 shows cross-plots for surface PO_4 concentration for the best-fit CBRU and the standard model for the selected ocean regions. The addition of temperature-dependence in CBRU generally increases the surface nutrient concentration and is in better agreement with data than the standard model. The high surface nutrient regions, Antarctic and the North Pacific, are lower than data in all model cases and this is likely due to the lack of iron limitation in this version of the model, as biological activity removes too much nutrient from the surface waters. In these regions, the temperature-dependent version shows slightly better fit to data than the standard model, as the colder surface water reduces nutrient uptake rates. However, the very lowest nutrient regions (e.g. some south Pacific and some west tropical Atlantic) are slightly higher compared to data for CBRU the temperature-dependent version.~~

Commented [m4]: Contrasting TDEP to CB should come under the following section …

4.2 Performance of the temperature-dependent model compared to the standard model

~~We~~In this section we evaluate and compare~~ contrast~~ the performance of the existing tuned, but non temperature-dependent ~~BIOGEM~~ biological scheme (~~CB~~STND), ~~with~~ to the new tuned temperature~~-~~ dependent scheme (~~CBRU~~TDEP).

Figure~~:~~ 6 shows cross-plots for surface PO_4 concentration (an important constraint on export production) for the best fit ~~CBRU~~TDEP and the standard model for the selected ocean regions. The addition of temperature dependence in ~~CBRU~~TDEP generally increases surface PO_4 concentrations and comes into better agreement with data than the standard model (~~CB~~STND). The high surface nutrient regions, Antarctic and the North Pacific, are lower than data in all model cases and this is likely due to the lack of iron limitation in this version of the model, as biological activity removes too much nutrient from the surface waters. However, in these regions, the temperature-dependent version shows a slightly better fit to data than does the standard model, as the colder surface water reduces nutrient uptake rates. In contrast, the ~~very~~ lowest nutrient regions (e.g. some south Pacific and some east~~west~~ tropical Atlantic) ~~are~~have slightly higher PO_4 concentrations compared to data in~~for~~ ~~CBRU~~TDEP ~~the temperature-dependent version~~.

Formatted: Subscript

Regional water-column profile model outputs for ~~CBRU~~TDEP and ~~CB~~STND are plotted against PO_4 ~~from WOA 2009~~data (Levitus et al. 2010) in Fig. 7. In both schemes, the model was tuned according to its fit to PO_4 (as well as O_2) and both ~~CBRU~~TDEP

and ~~CB~~STND show a visually ~~good~~ reasonable fit to data. Some differences can be seen between ~~CBRU~~TDEP and ~~CB~~STND in surface mid and low latitude waters, e.g. in the n~~N~~orth Indian Ocean and e~~E~~astern t~~T~~ropical Pacific, where nutrients are higher in ~~CBRU~~TDEP in better agreement with data. In higher latitude waters, model-data mismatch~~differences~~ may be more closely related to ocean circulation~~,~~ (as for temperature, ~~(~~Fig. 4)~~,~~ with ~~CB~~STND and ~~CBRU~~TDEP distribution very similar to each other in the Southern Ocean and North Pacific, but with and ~~CBRU~~TDEP ~~slightly~~ a better fit to data in the North Atlantic.

~~We find that~~ With the exception of the ~~very~~ high southern latitudes (higher than ~ 60°S), the~~the~~ addition of temperature-dependent microbial processes generally increases surface nutrient concentrations (as shown in Fig. 8 a and b) as compared to the standard model ~~(except for the very high southern latitudes)~~. This is ~~especially the case~~particularly apparent in the low-nutrient gyres, with up to 4-times higher PO_4 concentrations ~~present i~~in ~~CBRU~~TDEP ~~than~~ as compared to in~~in~~ ~~CB~~STND (Fig. 8b). In the deeper ocean (Fig 8 c and d), nutrient concentrations are ~~is~~ reduced in the temperature-dependent version except for in the North Atlantic (where higher surface nutrients are delivered to the deep via the AMOC) and the high Southern latitudes (with slightly higher PO_4 than the standard model).

The distribution of dissolved oxygen also provides important information about the biological pump. Photosynthesis removes CO_2 from ocean waters and adds O_2~~,~~ (where~~ich~~ CO_2 and O_2~~it~~ are~~is~~ also exchanged with the atmosphere at the surface ocean), ~~where~~ while respiration does the opposite. ~~In surface waters and the mixed layer, ventilation with the atmosphere also results in higher oxygen concentration.~~ As a general pattern, respiration progressively reduces dissolved oxygen concentrations down the water column until a minimum is reached. Below that depth – the 'oxygen minimum zone' (OMZ) – ocean circulation reintroduces more oxygenated water masses from below~~(ventilated from higher latitude and colder surface waters), slightly increasing d~~. Dissolved oxygen concentrations then slightly increase again with further depth as the flux of organic matter and hence respiration declines, and oxygen is supplied through deep ocean circulation and via ventilation at the poles. In the Antarctic zone (Fig. 9), circulation patterns appear to dominate oxygen content (as ~~CB~~STND and ~~CBRU~~TDEP are very similar, but fairly dissimilar to data indicators). The North Pacific region also shows offsets between model and data for O_2, PO_4 and temperature, also suggesting ~~a deficiencies~~deficiencies in simulated deep ocean circulation ~~difference~~~~controller~~. In low latitude waters, ~~CBRU~~TDEP shows a better fit to data between the surface and 500m than ~~CB~~STND, suggesting that oxygen depletion rates due to respiration are better described here. Overall, the intensity of the OMZ in both ~~CB~~STND and ~~CBRU~~TDEP ~~are~~ appear visually in reasonable agreement with data, although in low and mid latitudes warmer waters the OMZ occurs higher in the water column in ~~CBRU~~TDEP than ~~CB~~STND.

Formatted: Subscript

Formatted: Subscript

Commented [m5]: An odd sentence. It reads better without it.

4.3 Tracing Carbon-13

In studying paleo climates and, in particular, past states of ocean circulation and carbon cycling, c~~C~~arbon-13 data ~~are~~ is widely used as ~~indicators of ocean circulation and of changes in that circulation over time~~a tracer (Lynch-Stieglitz 2003). ~~Water~~ Surface~~masses~~ waters have characteristic carbon-13 signatures with a pronounced mostly latitudinal gradient, so changes in $\delta^{13}C$ measured at any one location on the ocean floor may be at least partially attributed to changes in the strength and location of deep-water formation ~~in the water sources~~. The biological pump also affects the $\delta^{13}C$ ~~of ocean waters~~signature of seawater. The process of photosynthesis fractionates the carbon that is exchanged (from the dissolved inorganic to the organic form); carbon-12 is preferentially taken up,

leaving more carbon-13 in the surface waters (Schmittner et al. 2013). As summarized by Kirtland Turner and Ridgwell (2016), in the cGENIE model, fractionation between POC (and DOC) and $\delta^{13}C$ of CO_2(aq) in cGENIE is a function of the CO_2(aq) concentration and based on an approximation of the model of Rau et al. (1996) (Ridgwell, 2001). This gives rise to a spatial distribution in the $\delta^{13}C$ of exported organic carbon, with lower (more negative values) at higher latitudes, and higher (less negative) values towards the equator, primarily reflecting the temperature control on the concentration of CO_2(aq) in surface waters. The mean flux-weighted $\delta^{13}C$ of POC is around -23‰ for the pre-industrial period, and around -26‰ by the year 2010 due to the impact of increasing CO_2(aq) on organic carbon ^{13}C fractionation as well as the Suess effect. As POC is remineralised in the water column, low $\delta^{13}C$ carbon is released ~~into the water~~, modifying the ambient $\delta^{13}C$ of DIC. The $\delta^{13}C$ of the ocean interior then represents a balance between the input of light $\delta^{13}C$ via the biological pump, and the ingress of heavier $\delta^{13}C$ supplied in deep waters and ultimately sourced from high latitudes at the surface.

The regional mean and standard deviation of data $\delta^{13}C$, and model ~~CBRU~~TDEP and ~~CB~~STND are shown in Fig. 10. For almost all regions, ~~general~~ the broad patterns are similar to those seen in dissolved O_2 concentration, ~~except the Antarctic zone. B~~~~with~~with benthic and deep ~~-~~ water absolute $\delta^{13}C$ values ~~are~~ generally similar to data for both model configuration~~setting~~s. One exception is the Antarctic zone ~~BLAH~~where $\delta^{13}C$ shows a good fit to data indicators nearer the surface, where modelled oxygen shows a poorer fit to data nearer the surface. ~~The model data~~The offset in mid-depth waters (~800m) in the sub-Antarctic zone may be due to a reduced Antarctic intermediate waters contribution in the model. This may also explain similar model-offsets at this depth in the South and East-Tropical Pacific regions. In warm surface waters, $\delta^{13}C$ reduces more quickly with depth in ~~CBRU~~TDEP than ~~CB~~STND, as nutrient recycling is occurring faster.

4.4 POC export and implications for biological carbon pump efficiency

The inclusion of a temperature ~~-~~ dependence term in remineralisation strongly affects both the export ~~production~~ of POM via ~~the~~ changes in the rate of nutrient recycling, ~~and fundamentally affects the~~as well as the efficiency of the biological carbon pump. To demonstrate the impact of each varied parameter, the export flux of POC (~~measured~~ modelled at 80m) for every simulation (not only the best-fit ~~CBRU~~TDEP) is shown in Fig. 11. With a lower activation energy requirement (low $E_a(1)$ value), less energy is needed for the remineralisation process to occur, this means nutrients are returned to surface waters more quickly, production is higher, and so POC flux at 80m is higher. Conversely, the higher the $E_a(1)$ value, the more energy is required to remineralise organic carbon. So, at higher $E_a(1)$, proportionally more organic carbon reaches depth making surface processes less important. The fraction of the POC exported that is recalcitrant and the maximum nutrient uptake rate at the surface becomes less important as $E_a(1)$ increases. This trend occurs because there is no variation in ocean temperature between runs in Figure 11 a), i.e., atmospheric CO_2 and climate are fixed. It is important to note however that a larger $E_a(1)$ leads to a larger sensitivity of remineralisation rates to changes in temperature, e.g., a higher Q_{10} (Fig. 11 b) and c)). The Q_{10} for remineralisation rates in Figure 11 ranges from below 2.3 ($E_a(1)$ = 53 kJ mol^{-1}) to over 2.5 ($E_a(1)$ = 60 kJ mol^{-1}) for a change in temperature from 0°C to 10°C (Fig. 11 c).

The remineralisation curves for each ocean region are~~is~~ shown in Fig. 12 for the best fit ~~CBRU~~TDEP and ~~CB~~STND model for POC (in gC m^{-2} yr^{-1}). ~~CBRU~~TDEP and ~~CB~~STND have differing initial POC export fluxes with lower latitude warmer waters

Formatted: Subscript
Formatted: Superscript

showing higher export in ~~CBRU~~TDEP due to the increased nutrient recycling there. A dataset of POC flux (Mouw et al. 2016a) is overlaid on the remineralisation curves (Fig. 12). In both model configurations, the measured Antarctic zone POC flux at shallow and intermediate depths (< 1500m) is significantly lower than in the model. We do not ~~apply~~ account for iron limitation in the Southern Ocean (or elsewhere) in this particular configuration of the cGENIE model, which would tend to act to limit productivity and POC export there~~,~~ and hence could potentially explain some of the mismatch we observe at shallower depths. ~~However~~In general, the measured flux at depth appears ~~well~~ reasonably represented with the exception of warmer regions~~.~~, where the ~~In deeper waters elsewhere,~~ measured POC flux ~~in warmer regions~~ (e.g. ~~e~~East tropical Pacific, North Indian, ~~e~~East Tropical Atlantic) is generally higher than in the model. This likely reflects additional processes that may increase POC fluxes to depth such as ballasting by minerals (Klaas and Archer, 2002; Wilson et al 2012) and the lower reactivity of POC associated with increased recycling in low latitude plankton ecosystems (Aumont et al., 2017).

Overall, the pattern of the efficiency of the transfer of particles from 80m to 1040m (Fig. 13) in ~~CBRU~~TDEP is similar to that found in Weber et al. (2016), where efficiency of transfer is essentially a measure of the rate of remineralistion; what fraction of the POC exported at 80m that reaches 1040m. Colder waters show higher transfer efficiency, with the lowest transfer efficiency seen in the sub-tropical gyres. The ~~CB~~STND model has a fixed decay rate for all locations, so the transfer efficiency at any particular depth has a global uniform value. The global export-weighted mean remineralisation depth for STND is 627m, and for TDEP 378m ± 236m.

It should be noted that here we have included all available data from Mouw et al. (2016a) without any attempt to ensure these data are representative of the annual mean (where the model output represents the annual mean). POC flux measurements can be highly dependent on time of year and number of data measurement points available. Some of the model-data mismatch may then be due to a mis-match between the interval in time represented by the data, and the annual mean of the model. For instance, blooms, which are not well represented in the model, may explain some of the very high POC flux values (for example 0.2 gC m^{-2} yr^{-1}) in the North Atlantic and hence why the model annual mean appears to underestimate the flux.

5 Implications of including temperature-dependent microbial processes

5.1 The role of temperature in the marine carbon cycle response to historical warming

~~This temperature-dependent~~ enhanced ~~version of the cGENIE model treats~~ ~~focusses~~In this study we have focussed on the two~~2~~ main components~~two large-scale processes~~ of the biological carbon pump. Firstly, nutrient uptake rates due to the metabolic temperature~~-~~ dependence of photosynthesising marine biota; secondly remineralisation rates of sinking particulate organic matter due to the metabolic temperature~~-~~ dependence of respiring marine biota feeding on that sinking organic matter. We find that t~~T~~he calibrated temperature response of the respiration-based mechanism of remineralisation in the water column is more sensitive to temperature change (a mean *Q10* of 2.~~28~~ 28 over a range of temperatures from 0°C to 26°C, from Eq.5 using 54 kJ mol^{-1} for E_a*(1)*) than the photosynthesis-based one (the Eppley curve has a *Q10* of 1.88, in Eq. 3 and 4, Bissinger et al. 2008), in agreement with fundamental studies (Brown 2004). Historical temperature rise, which we induced in the cGENIE.muffin Earth system model by prescribing the observed CO_2 ~~transient~~ in the atmosphere, provides an illustrative example of the role and importance of including sufficient temperature-dependent processes in models. In this section we therefore discuss in more detail the transient differences between ~~CB~~STND and ~~CBRU~~TDEP model configurations.

Between the years 1700 and 2010, global mean air temperature in cGENIE increases by 0.94°C. In turn, warming at the ocean surface induces stratification in the water column, reducing nutrient re-supply to the surface from subsurface waters. In the ~~CB~~STND model, this results in a pronounced drop in POC export at 80m of 2.9% (Fig. 14), in agreement with the average of the CMIP5 models (Bopp et al., 2013). ~~. In CBRU this effect is largely offset by the intensified recycling of nutrients in warmer surface and near-surface waters.~~ However, the transfer efficiency is additionally affected in ~~CBRU~~TDEP, with a drop of over 5% in the proportion of POC exported at 80m that reaches 1040m (equivalent to a shoaling of the global mean remineralisation depth of 16m) (Fig 15). ~~The largest transfer efficiency drops are seen in low and mid latitude waters (Fig. 15).~~ This reduction in biological pump transfer efficiency is a result of increased rates of remineralisation in the warming water column, principally in surface and near-surface waters (while whole~~, (~~volumetrically-weighted~~,)~~ ocean warming is 0.12°C over this period, 0.6°C occurs on a global mean basis in surface waters, and 0.02°C in deepest waters). The result is that for TDEP this stratification-induced nutrient-limitation effect on export is largely offset by the intensified recycling of nutrients in warmer surface and near-surface waters.

Between ~~simulation~~ simulated pre-industrial and present-day model states, we found a ~~significantly~~ substantially smaller drop in POC flux at 80m when temperature dependence was included (~~CBRU~~TDEP) compared to the standard model (~~CB~~STND). Global POC flux at 80m reduces by 0.3% between pre-industrial and present-day in ~~CBRU~~TDEP, but with increases in the Southern Ocean of around 10% and in the tropics of around 1%, suggesting an increase in NPP (Net Primary Productivity) in the tropics. Kwiatkowski et al. (2017) identified a reduction in NPP with warming in the tropical ocean of 3±1% per degree of warming, based on responses to ENSO (El Nino Southern Oscillation) which ~~is~~ on face value is inconsistent with our simulation of a possible increase in NPP in the tropics. Their estimate utilised satellite based NPP products from data on chlorophyll and light incidence, and they found that in no data-constraint did NPP increase in the tropics (although the data constraint varied according to the NPP product used). However, Behrenfeld et al. (2015) noted that a reduction in chlorophyll does not necessarily represent a reduction in

productivity, due to photoacclimation. The satellite based NPP products do not account or correct for this effect, so may well underestimate NPP in warming conditions. In an earlier study, Taucher and Oschlies (2011) found an increased NPP when temperature dependence was included in modelled future projections. Laufkotter et al. (2017) also found that when including a temperature-dependence and oxygen content-dependent remineralisation, NPP increased on warming due to intensified nutrient recycling in near-surface water. However, ~~T~~they suggested this was largely due to an initial positive bias in surface ocean nutrients. In a second model set-up, they reduced nutrient recycling in surface waters and find little impact on NPP between the temperature sensitive and temperature independent model in a future projection to 2100 CE.

In this study we make no distinction between dissolved oxygen and sulphate in terms of controlling the remineralisation rate of POC (~~BLAH~~unlike, for instance, Laufkotter et al. 2017). Cavan et al (2017) concluded that the large oxygen minimum zone in the Eastern Tropical Pacific reduces the rate of remineralisation due to the almost complete absence of zooplankton particle disaggregation within, and provides a negative feedback to warming. However, Cram et al. (2018) explained ~~M~~most of the regional variability in the flux of POC in the deep sea ~~was explained~~ via particle size and the effect of temperature on remineralisation ~~remineralisation in a study by Cram et al. (2018)~~, with oxygen concentration providing ~~only~~ a small improvement (by reducing nutrient recycling in the Eastern Tropical Pacific). ~~Cavan et al (2017) concluded that the large oxygen minimum zone in the Eastern Tropical North Pacific reduces the rate of remineralisation due to the almost complete absence of zooplankton particle disaggregation within, and provides a negative feedback to warming.~~ Particle size plays a role in sinking speeds, as larger particles sink faster (generally), and particle size is a factor in export and transfer efficiency (Mouw et al 2016b). The ~~version~~ configuration of cGENIE we ~~used~~ employ here does not account for particle size and has a fixed sinking speed globally (by default, 125 m d^{-1}). The lack of particle size variability and oxygen concentration's role in remineralisation may explain some of the increased POC flux at 80m that the model shows since the pre-industrial period in tropical waters. This tropical~~s~~ POC export increase may also be partly due to initial higher nutrient concentrations compared to data, or to the increased remineralisation rates re-supplying nutrients to the surface, but may also be linked to changes in DOM cycling (see section 5.2). ~~In summary, projected and p~~Predicted changes (and changes that may have already occurred) in NPP in low-nutrient warm waters are still subject to large uncertainties (Turner et al. 2015, Cross et al. 2015).

There is also still uncertainty as to the causes, and even patterns, in POC flux differences ~~in~~ across different ocean regions (Henson et al., 2012; Marsay et al., 2015; Weber et al., 2016; Cram et al., 2018). We find the patterns of transfer efficiency (Fig. 13) for ~~CBRU~~TDEP are in broad agreement with Marsay et al. (2015) and Weber et al. (2016). This transfer efficiency is not dependent on surface waters NPP patterns or on how much POC is exported at 80m in cGENIE, however, the absolute amount of carbon reaching the deep ocean does depend on NPP and export. On warming since the pre-industrial period we found a reduced POC flux at 80m as well as a reduction in transfer efficiency, combining to produce a reduction in the strength of the biological carbon pump with warming. This further implies an increased carbon pump strength in cooler climates, as per Heinze et al. (2016).

We note that- circulation states and upwelling/downwelling changes can also have an impact on the distribution of carbon, oxygen and nutrients between the surface and the deep (Kvale et al 2019, Loptien and Dietze 2019), and are also model-dependent. ~~, however~~ Ccirculation changes are ~~very~~ small between the pre-industrial and the present-day compared to the simulations in Kvale

et al (2019) where very high CO_2 (up to 1200ppm) and high surface temperature results in large ocean circulation pattern changes; increased nutrient storage in the deep ocean was due to longer residence time of deep ocean water in that study (see Chikamoto et al. 2008 for the effect of Atlantic Overturning Circulation shutdown in cGENIE). In our study we have found that the temperature-dependent biological pump offsets some of the effects of physical ocean response to warming (in increased near-surface nutrient recycling, so offsetting the effect of increased ocean stratification that otherwise reduces surface nutrients in the STND simulation). However, this is not to suggest that a temperature-dependent biological pump could offset the effect of extreme changes in circulation, such as an AMOC shutdown, or for far more extreme warming scenarios than that applied here. We do not test such scenarios here. ~~compared to the effect of metabolic temperature dependence.~~

5.2 Temperature and the cycle of dissolved organic matter in the ocean

In this paper and associated model calibration, we have focussed on the role of temperature in the production and fate of POM. However, the relative partitioning of primary production into DOM (rather than POM) together with its mean residence time at (or close to) the ocean surface, modulates nutrient recycling. Temperature-sensitivity of these 2 processes thereby adds an additional set of feedbacks between ~~temperature~~climate and the biological carbon pump.

~~Conceptually, the fate of DOM is relatively easy to address as in theory, it should display an analogous temperature-dependent response as per POM. In the standard configuration of the cGENIE Earth system model (e.g. as per Ridgwell et al., 2007; Cao et al., 2009), the lifetime of DOM is fixed and set at a value of 0.5 years following Najjar et al. [2007].~~ To explore the wider role of temperature in the marine carbon cycle ~~including that of DOM, we also now implement,~~and as a further option in the model, ~~the same~~we add a similar temperature~~-~~dependence to the remineralis~~z~~ation of DOM as for POM (Equation 5):

$$k(T)_{DOM} = \beta A_{DOM} e^{\left(-E_a/RT\right)} \quad (7)$$

where E_a is the activation energy and is assigned a value of 54000 J mol^{-1}, and R and T are the gas constant (J K^{-1} mol^{-1}) and absolute temperature (K), respectively. $k(T)_{DOM}$ is the rate constant ($year^{-1}$) controlling the decay of DOM and replaces the previous fixed lifetime value of 2.0 $year^{-1}$.

~~Assuming~~The assumption that the same activation e~~n~~ve~~r~~gy applies to DOM as ~~per~~ for POM (~~that was calibtrated in conjunction with an assumed sinking rate of POM of 125 m d^{-1}), leads to a calibrated value of A in Eq. 5 (9.0×10^{11}). However, implementing Eq. 7 with~~i.e. setting β_{DOM} = 9.0 x 10^{11} in Eq. 7) l~~ead~~s~~ to a global mean DOM lifetime of approximately 0.02 years, compared to the value of 0.5 years in the standard model (Ridgwell et al., 2007) that follows Naijar et al. (2007). This might: (i) reflect a different mean quality (~~reactivity~~and hence a different activation energy) of~~to~~ the organic matter assumed to constitute DOM as opposed to POM;~~,~~ and/or~~,~~ (ii) reflect the dispersed nature of DOM versus the more concentrated POM and/or differences in the associated bacterial biomass;~~,~~ and/or (iii) that the assumed sinking speed of 125 m d^{-1} is simply too unrealistically fast ~~fast an assumption~~. ~~While one could argue that (i) also may imply that a different activation energy for DOM is also required.~~ However, to simplify ~~and linearize~~ the model re-tuning of the DOM cycle, we only adjust the value of β_{DOM}. For a

Formatted: Font: Italic

fixed production fraction of 0.66, setting β_{DOM} = 1.16 x 10^{10} g ~~$A_{DOM} = 1.16 \times 10^{10}$~~ gives a mean (flux weighted) DOM lifetime in the model that matches~~ing~~ the fixed 0.5 year value of the original model configuration.

The production of DOM (vs. POM) is also likely to be influenced by ambient temperature. Dunne et al. (~~[~~2005~~]~~) describe a multiple linear regression analysis of observed ocean surface properties, as well as primary and export production, across a range of different ocean environments, and deduce a role for sea surface temperature in predicting the observed particle export ratio. Although the Dunne et al. (~~[~~2005~~]~~ regression based on temperature and net primary productivity has previously been employed by Ma and Tian ~~[~~(2014)~~]~~ to formulate the production of DOM vs. POM (and co-incidentally, also in a version of the cGENIE Earth system model), the default biological scheme of 'induced fluxes' (~~[~~Maier-Reimer, 1993)~~]~~ does not provide a value of primary productivity — required by the regression model. Additionally, the default configuration of the ocean circulation model does not calculate a mixed layer depth – required to convert between units for primary production in the regression formula. ~~(~~Dunne et al. (~~[~~2005)~~]~~ also provide an alternative and slightly improved regression model ~~is~~ based on mixed layer Chl*a* concentrations (and temperature), but this would require use of the Ward et al. (~~[~~2018)~~]~~ 'ECOGEM' ecological model component in the cGENIE Earth system model, and outside the scope of this present study.~~)~~

Rather than attempt to ~~recalculate~~reformulate (and re-fit) the Dunne et al. (~~[~~2005)~~]~~ regression model ~~of the particle export ratio using~~as a function of the environmental parameters simulated by the cGENIE model, we simply extract the temperature sensitivity term in isolation (while recognising that is was derived by Dunne et al. (~~[~~2005)~~]~~ jointly alongside primary production (or Chl*a*~~)~~) in order to derive a temperature-dependent ~~n~~ equation for the partitioning of POM vs. total organic matter export (DOM+POM), γ:

$$\gamma = \text{~~}a - bT - c - dT \quad for\ 0.04 < \gamma < 0.72 \qquad (8)$$

where ~~b~~$_d$ is the temperature sensitivity of 0.0101 °C^{-1} from Dunne et al. (~~[~~2005)~~]~~, and ~~a~~$_C$ is a constant (0.512), whose value is chosen such that the global mean (production-weighted) export of DOM vs. POM occurs in a 2:1 ratio (i.e. γ = 0.34).

This completes the implementation of an option for temperature-dependency in both the creation and remineralis~~z~~ation of DOM, with the exception that the two~~2~~ parameteris~~z~~ations interact, and in order to configure~~ation~~ cGENIE such that the mean production fraction of DOM and mean lifetime both align with the values (0.66 and 0.5 years, respectively) in the original model (i.e. Ridgwell et al., 2007; Cao et al., 2009), we make a final adjustment to: β_{DOM} = 1.32 x 10^{10} (and keeping the initial calibrated value of a = 0.512 in Eq. 8).

A further simulation (a pre-industrial spin-up followed by a transient simulation forced by CO_2 and $\delta^{13}CO_2$ data-indicated changes from 1700 to the year 2010) - called TDEP$_{\gamma TDOM}$ - was conducted that includes the best fit TDEP parameters but now adds the temperature-dependent production and decay of DOM as described above. For the present day, TDEP$_{\gamma TDOM}$ slightly improves the model fit to oxygen distribution compared to TDEP, with lower CRMSD and higher correlation, whilst model fit to PO_4 is slightly worsened (Table 4).

Formatted: Superscript
Formatted: Font: Not Italic
Formatted: Not Highlight
Formatted: Not Highlight
Formatted: Not Highlight
Formatted: Font: Italic
Formatted: Font: Italic, Subscript
Formatted: Superscript
Formatted: Subscript
Formatted: Superscript
Formatted: Subscript
Formatted: Subscript
Formatted: Subscript
Formatted: Subscript

The inclusion of temperature-dependent DOM processes also affects the response of ocean carbon cycling to historical warming. The global mean export-weighted remineralisation depth for the present-day in $TDEP_{+TDOM}$ is 399m +- 255m (21m deeper than TDEP), and the change in depth since 1700 is a shallowing of 16m (the same as for TDEP). Slightly less POC is exported at 80m in $TDEP_{+TDOM}$ compared to TDEP by 2010 (Fig.14), indicating that although increases in surface nutrient recycling (due to temperature-dependent POC processes) significantly offsets the effects of warming-induced ocean stratification in TDEP, this is counterbalanced but to a lesser extent by temperature dependence in DOM production and remineralisation in $TDEP_{+TDOM}$.

In response to warming and compared to STND and TDEP, $TDEP_{+TDOM}$ exhibits a slightly increased global DOM production ratio (the fraction of organic matter produced that is dissolved rather than particulate, as Fig 1) driven by temperature-dependent DOM production (table 5). This is countered, however, with a (global) shorter DOM lifetime at the surface driven by temperature-dependent DOM remineralisation. The net result is a decline of 0.74% in the mean global surface DOM concentration between 1700 and 2010 CE in $TDEP_{+TDOM}$. In comparison, there is an increase of 0.54% in mean global surface DOM concentration for TDEP and a decrease of 2.07% in STND (Tables 5 and 6).

Appendix figures A1 and A2 provide a view of the spatial changes in DOM dynamics taking place between 1700 and 2100, and for each DOM process being individually temperature-enabled as well as both together. A summary is that the effect of temperature-dependent DOM is to increase the DOM production ratio in low latitudes, and decrease the production ratio in high latitudes compared to TDEP, with historical warming resulting in a general increase in DOM production between 1700 and 2010 in $TDEP_{+TDOM}$. The $TDEP_{+TDOM}$ DOM lifetime at the surface is decreased in low latitudes and increased in high latitudes compared to TDEP, with a general decrease in DOM lifetime in response to historical warming, and more pronounced in higher latitudes. $TDEP_{+TDOM}$ has lower surface DOM concentrations in the tropics compared to TDEP in the present day. Since 1700, surface DOM concentration has increased in the southern high latitudes in all model configurations, but $TDEP_{+TDOM}$ results in a slight decreased surface DOM concentration in the tropics, compared to a slight increase in TDEP.

Overall, the combined effects of temperature-dependent POM and DOM processes still results in a smaller reduction in modelled POC export at 80m compared to STND (Fig. 14 a) of 0.7% since 1700, although when only POM processes are enable as temperature-dependent, the decrease is smaller still (0.3%). Compared to TDEP: the $TDEP_{+TDOM}$ shows lower export production in mid and high latitudes (Fig. 14 b) but affects almost no change in transfer efficiency of the biological pump (Fig 15).

Formatted: Justified, Indent: First line: 1.27 cm, Line spacing: 1.5 lines
Formatted: Subscript
Formatted: Subscript
Formatted: Subscript
Formatted: Indent: First line: 1.27 cm
Formatted: Subscript
Formatted: Subscript
Formatted: Subscript
Formatted: Subscript
Formatted: Justified, Indent: First line: 1.27 cm, Line spacing: 1.5 lines

6 Summary

~~Substituting temperature-dependent organic matter export and remineralisation parameterisations into cGENIE.muffin, changes patterns of nutrient PO_4, dissolved oxygen, and carbon-13 distributions in the ocean compared to the standard model.~~ The STND and TDEP variants~~Although both, model variants (original, and that presented in this paper)~~ of the cGENIE.muffin model are tuned ~~in some way~~ to observed PO_4 and O_2 distributions and achieve comparable statistical fits to ocean climatologies. However,~~,~~ substituting temperature-dependent~~ particulate organic matter~~ particulate organic matter (POM) export and remineralisation parameterisations into cGENIE.muffin~~,~~ changes the patterns of PO_4, dissolved oxygen, and carbon-13 distributions in the ocean compared to the standard model, and ~~and leads to s~~substantive differences between models occur in response to warming since the pre-industrial period. ~~In~~ Specifically,~~:~~ in response to warming, inclusion of a temperature-dependence~~y~~ on the production and remineralis~~z~~ation of ~~particulate organic matter (POM)~~POM increases the efficiency of nutrient and carbon recycling to the surface. In the case of a transient and geologically-rapid warming, this temperature-driven increase in recycling is sufficient to largely offset a decrease in nutrient re-supply due to enhanced physical stratification of the upper ocean, leaving global POM export relatively unaffected by historical warming. ~~ameliorates stratification-induced surface nutrient limitations by increasing nutrient recycling nearer to the surface. As a corollary, less carbon and nutrients are delivered to the deep. On cooling, the inverse is expected with more nutrients and carbon reaching depth, and a more efficient ocean carbon pump. Hence temperature-dependency of the biological pump may act as a positive feedback on atmospheric CO_2 concentrations and climate change.~~ Additionally accounting for temperature-dependency in both the production and remineralisation of dissolved organic matter (DOM) further modifies the global carbon cycle response to historical warming, but to a much lesser extent than did the inclusion of POM-linked processes. Finally, the temperature-dependent biological pump results in a large reduction in the efficiency of the transfer of carbon from the surface to the deep ocean over the historical period simulation compared to the standard model.

Appendix A, Further information on the temperature-dependent DOM

Formatted: Heading 1

We combined the processes of temperature-dependent uptake and remineralisation for the POC driven biological pump as each process has been individually applied in previous published work. However, for the newly developed temperature-dependent DOM processes we show here (for each model configuration discussed in the text) the separate effects of temperature-dependent DOM production and temperature-dependent DOM remineralisation mapped as global surface distributions for: DOM production ratio, DOM lifetime, and DOM surface concentration (Fig A1). We further show for each parameter the anomaly at 2010 with respect to the year 1700 (Fig A2).

7 Model code availability

The specific version used of the cGENIE.muffin model used in this paper is tagged as release v0.9.1237, and has been assigned a DOI: 10.5281/zenodo.3999080~~DOI: 10.5281/zenodo.3559853~~. The code is hosted on GitHub and can be obtained by cloning:

https://github.com/derpycode/cgenie.muffin

changing the directory to cgenie.muffin and then checking out the specific release:

$ git checkout v0.9.1237

Configuration files for the specific experiments presented in the paper can be found in the directory:

genie-userconfigs\MS\crichtonetal.GMD.~~2019~~2020

Commented [CK6]: Need to change?

Details of the experiments, plus the command line needed to run each one, are given in the readme.txt file in that directory. All other configuration files and boundary conditions are provided as part of the release.

A manual, detailing code installation, basic model configuration, plus an extensive series of tutorials covering various aspects of muffin capability, experimental design, and results output and processing, is provided on GitHub. The latex source of the manual, along with pre-built PDF file can be obtained, by cloning:

https://github.com/derpycode/muffindoc

~~The muffin manual contains instructions for obtaining, installing, and testing the code, plus how to run experiments. Specifically:~~

~~Section 1.1 (Installation, configuration, basic usage) – Provides a basic over-view of the software environment required for installing and running muffin.~~

~~Section 1.2.2 – provides a basic over-view of cloning and testing the code.~~

~~Section 1.3 – Provides a basic guide to running experiments (also see 1.6 and 1.7).~~

~~Section 1.4 – provides a basic introduction to model output (much more detail is given in Section 12).~~

~~HOW-TO Chapter – Provides a detailed guide to cloning the code and configuring both an Ubuntu (18.04) and a, MacOS, and Windows software environments, including netCDF library installation, plus running a basic test.~~

Author contribution

KAC ~~set up~~devised, ran and analysed the model ensemble and data, JDW and AR developed the temperature~~-~~ dependent remineralisation process, AR developed the temperature-dependent DOM processes, all authors wrote the manuscript.

Acknowledgments

KAC was supported by Natural Environment Research Council (NERC) grant number NE/N001621/1 to PNP. JDW was supported by the European Research Council as part of the "PALEOGENiE" project (ERC-2013-CoG-617313). AR acknowledges additional support from the National Science Foundation under Grants 1702913 and 1736771.

References

Arndt, S., Jørgensen, B.B., LaRowe, D.E., Middelburg, J.J., Pancost, R.D. and Regnier, P.: Quantifying the degradation of organic matter in marine sediments: a review and synthesis, Earth-Sci. Rev., 123, 53-86, doi: /10.1016/j.earscirev.2013.02.008, 2013

Aumont, O., van Hulten, M., Roy-Barman, M., Dutay, J.-C., Éthé, C., and Gehlen, M.: Variable reactivity of particulate organic matter in a global ocean biogeochemical model, Biogeosciences, 14, 2321–2341, doi:10.5194/bg-14-2321-2017, 2017

Bach, L.T., Boxhammer, T., Larsen, A., Hildebrandt, N., Schulz, K.G. and Riebesell, U.: Influence of plankton community structure on the sinking velocity of marine aggregates, Global Biogeochem. Cy., 30(8), 1145-1165, doi:10.1002/2016GB005372, 2016.

Behrenfeld, M.J., O'Malley, R.T., Boss, E.S., Westberry, T.K., Graff, J.R., Halsey, K.H., Milligan, A.J., Siegel, D.A. and Brown, M.B.: Revaluating ocean warming impacts on global phytoplankton, Nat. Clim. Change, 6(3), 323-330, doi: 10.1038/nclimate2838, 2016.

Bendtsen, J., Hilligsøe, K.M., Hansen, J.L. and Richardson, K.: Analysis of remineralisation, lability, temperature sensitivity and structural composition of organic matter from the upper ocean, Prog. Oceanogr., 130, 125-145, doi: 10.1016/j.pocean.2014.10.009, 2015.

Bissinger, J.E., Montagnes, D.J., harples, J. and Atkinson, D.: Predicting marine phytoplankton maximum growth rates from temperature: Improving on the Eppley curve using quantile regression, Limnol. Oceanogr., 53(2), 487-493, doi: 10.4319/lo.2008.53.2.0487, 2008.

Bopp, L., Resplandy, L., Orr, J.C., Doney, S.C., Dunne, J.P., Gehlen, M., Halloran, P., Heinze, C., Ilyina, T., Seferian, R. and Tjiputra, J.: Multiple stressors of ocean ecosystems in the 21st century: projections with CMIP5 models. Biogeosciences, 10, 6225-6245, doi: 10.5194/bg-10-6225-2013, 2013.

Boscolo-Galazzo, F., Crichton, K.A., Barker, S. and Pearson, P.N.: Temperature dependency of metabolic rates in the upper ocean: A positive feedback to global climate change?, Global Planet. Change, 170, 201-212, doi: 10.1016/j.gloplacha.2018.08.017, 2018.

Boyd, P.W., Claustre, H., Levy, M., Siegel, D.A. and Weber, T.: Multi-faceted particle pumps drive carbon sequestration in the ocean, Nature, 568, 327-335, doi:10.1038/s41586-019-1098-2, 2019.

Brown, J.H., Gillooly, J.F., Allen, A.P., Savage, V.M. and West, G.B., 2004. Toward a metabolic theory of ecology. Ecology, 85(7), pp.1771-1789.

Burd, A.B., Frey, S., Cabre, A., Ito, T., Levine, N.M., Lønborg, C., Long, M., Mauritz, M., Thomas, R.Q., Stephens, B.M. and Vanwalleghem, T.: Terrestrial and marine perspectives on modeling organic matter degradation pathways. Global change biology, 22, 121-136, doi: 10.1111/gcb.12987, 2016.

Cao, L., Eby, M., Ridgwell, A., Caldeira, K., Archer, D., Ishida, A., Joos, F., Matsumoto, K., Mikolajewicz, U., Mouchet, A., Orr, J.C., Plattner, G.K., Schlitzer, R., Tokos, K., Totterdell, I., Tschumi, T., Yamanaka, Y., Yool, A.: The role of ocean transport in the uptake of anthropogenic CO2, Biogeosciences, 6, 375–390, doi: 10.5194/bg-6-375-2009, 2009.

Cao, L. and Zhang, H.: The role of biological rates in the simulated warming effect on oceanic CO2 uptake, J. Geophys. Res.-Biogeo., 122(5), pp.1098-1106, doi: 10.1002/2016JG003756, 2017.

Cavan, E.L., Trimmer, M., Shelley, F. and Sanders, R.: Remineralization of particulate organic carbon in an ocean oxygen minimum zone, Nature Comms., 8, 14847, doi: 10.1038/ncomms14847, 2017.

Chikamoto, M.O., Abe-Ouchi, A., Oka, A. and Smith, S.L.: Temperature-induced marine export production during glacial period, Geophys. Res. Lett., 39, doi: 10.1029/2012GL053828, 2012.

Chikamoto, M. O., K. Matsumoto, and A. Ridgwell.: Response of deep-sea CaCO3 sedimentation to Atlantic meridional overturning circulation shutdown, J. Geophys. Res. Biogeosci. 113, G03017, doi:10.1029/2007JG000669, 2008.

Cram, J.A., Weber, T., Leung, S.W., McDonnell, A.M., Liang, J.H. and Deutsch, C.: The role of particle size, ballast, temperature, and oxygen in the sinking flux to the deep sea, Global Biogeochem. Cy., 32(5), 858-876, doi: 10.1029/2017GB005710, 2018.

Cross, W.F., Hood, J.M., Benstead, J.P., Huryn, A.D. and Nelson, D.: Interactions between temperature and nutrients across levels of ecological organization, Glob. Change Bio., 21(3), 1025-1040, doi: 10.1111/gcb.12809, 2015.

Dunne, J. P., Armstrong. R.A., Gnanadesikan. A.,, and Sarmiento. J.L.: Empirical and mechanistic models for the particle export ratio, Global Biogeochem. Cycles, 19, GB4026, doi:10.1029/2004GB002390. 2005.

Eppley, R.W.: Temperature and phytoplankton growth in the sea, Fish. bull, 70(4), 1063-1085, 1972.

Francey, R.J., Allison, C.E., Etheridge, D.M., Trudinger, C.M., Enting, I.G., Leuenberger, M., Langenfelds, R.L., Michel, E. and Steele, L.P.: A 1000-year high precision record of δ13C in atmospheric CO2. Tellus B, 51(2), 170-193, doi: 10.3402/tellusb.v51i2.16269, 1999

Edwards, N.R. and Marsh, R.: Uncertainties due to transport-parameter sensitivity in an efficient 3-D ocean-climate model, Clim. Dynam., 24(4), 415-433, doi: 10.1007/s00382-004-0508-8, 2005.

Heinze, C., Hoogakker, B.A. and Winguth, A.: Ocean carbon cycling during the past 130,000 years-a pilot study on inverse paleoclimate record modelling, Clim. Past, 12, 1949–1978, doi: 10.5194/cp-12-1949-2016, 2016.

Heinze, C., Meyer, S., Goris, N., Anderson, L., Steinfeldt, R., Chang, N., Le Quéré, C. and Bakker, D.C.: The ocean carbon sink-impacts, vulnerabilities and challenges, Earth Syst. Dynam., 6(1), 327, doi: 10.5194/esd-6-327-2015, 2015.

Henson, S.A., Sanders, R. and Madsen, E.: Global patterns in efficiency of particulate organic carbon export and transfer to the deep ocean, Global Biogeochem. Cy., 26(1), doi: 10.1029/2011GB004099, 2012.

Holden, P.B., Edwards, N.R., Fraedrich, K., Kirk, E., Lunkeit, F. and Zhu, X.: PLASIM–GENIE v1. 0: a new intermediate complexity AOGCM, Geosci. Model Dev., 9, 3347-3361, doi: 10.5194/gmd-9-3347-2016, 2016.

Hülse, D., Arndt, S., Wilson, J.D., Munhoven, G. and Ridgwell, A.: Understanding the causes and consequences of past marine carbon cycling variability through models, Earth-Sci. Rev., 171, 349-382, doi: 10.1016/j.earscirev.2017.06.004, 2017.

John, E.H., Wilson, J.D., Pearson, P.N. and Ridgwell, A.: Temperature-dependent remineralization and carbon cycling in the warm Eocene oceans, Palaeogeogr. Palaeocl., 413, 158-166, doi: 10.1016/j.palaeo.2014.05.019, 2014.

Keeling, C.D.: The Suess effect: 13Carbon-14Carbon interrelations, Environ. Int., 2(4-6), 229-300, doi: 10.1016/0160-4120(79)90005-9, 1979.

Formatted: Indent: First line: 0 cm

Kirtland Turner, S. and Ridgwell, A.: Development of a novel empirical framework for interpreting geological carbon isotope excursions, with implications for the rate of carbon injection across the PETM, Earth Planet. Sc. Lett., 435, 1-13., doi: 10.1016/j.epsl.2015.11.027, 2016.

Klaas, C. and Archer, D.E.: Association of sinking organic matter with various types of mineral ballast in the deep sea: Implications for the rain ratio. Global Biogeochem. Cy., 16(4), 63-1-14, doi: 10.1029/2001GB001765, 2002.

Kvale, K.F., Meissner, K.J. and Keller, D.P.: Potential increasing dominance of heterotrophy in the global ocean. Environ. Res. Lett., 10(7), 074009, doi:10.1088/1748-9326/10/7/074009, 2015.

Kvale, K.F., Turner, K., Landolfi, A. and Meissner, K.: Phytoplankton calcifiers control nitrate cycling and the pace of transition in warming icehouse and cooling greenhouse climates. Biogeosciences, 16(5), 1019-1034, doi: 10.5194/bg-16-1019-2019, 2019.

Kwiatkowski, L., Bopp, L., Aumont, O., Ciais, P., Cox, P.M., Laufkötter, C., Li, Y. and Séférian, R.: Emergent constraints on projections of declining primary production in the tropical oceans, Nat. Clim. Change, 7(5), 355-358, doi: 10.1038/nclimate3265, 2017.

Laufkötter, C., John, J.G., Stock, C.A. and Dunne, J.P.: Temperature and oxygen dependence of the remineralization of organic matter, Global Biogeochem. Cy., 31(7), 1038-1050, doi: 10.1002/2017GB005643, 2017.

Laufkötter, C., Vogt, M., Gruber, N., Aumont, O., Bopp, L., Doney, S.C., Dunne, J.P., Hauck, J., John, J.G., Lima, I.D. and Seferian, R.: Projected decreases in future marine export production: the role of the carbon flux through the upper ocean ecosystem, Biogeosciences, 13, 4023-4047, doi: 10.5194/bg-13-4023-2016, 2016.

Legendre, L., Rivkin, R.B., Weinbauer, M.G., Guidi, L. and Uitz, J.: The microbial carbon pump concept: Potential biogeochemical significance in the globally changing ocean, Prog. Oceanogr., 134, 432-450, doi: 10.1016/j.pocean.2015.01.008, 2015.

Levitus, S., Locarnini, R.A., Boyer, T.P., Mishonov, A.V., Antonov, J.I., Garcia, H.E., Baranova, O.K., Zweng, M.M., Johnson, D.R. and Seidov, D.: World ocean atlas 2009. National Oceanographic Data Center (U.S.), Ocean Climate Laboratory, United States, National Environmental Satellite, Data, and Information Service, 2010.

Löptien, U. and Dietze, H.: Reciprocal bias compensation and ensuing uncertainties in model-based climate projections: pelagic biogeochemistry versus ocean mixing, Biogeosciences, 16(9), 1865-1881, doi: 10.5194/bg-16-1865-2019, 2019.

Lynch-Stieglitz, J.: Tracers of past ocean circulation, Treatise on geochemistry, 6, 433-451, doi: 10.1016/B0-08-043751-6/06117-X, 2003.

Ma, W. and Tian, J., 2014. Modeling the contribution of dissolved organic carbon to carbon sequestration during the last glacial maximum. Geo-Marine Letters, 34(5), 471-482, doi: 10.1007/s00367-014-0378-y, 2014.

Mari, X., Passow, U., Migon, C., Burd, A.B. and Legendre, L.: Transparent exopolymer particles: Effects on carbon cycling in the ocean, Prog. Oceanogr., 151, 13-37, doi: 10.1016/j.pocean.2016.11.002, 2017.

Marsay, C.M., Sanders, R.J., Henson, S.A., Pabortsava, K., Achterberg, E.P. and Lampitt, R.S.: Attenuation of sinking particulate organic carbon flux through the mesopelagic ocean, P. Natl. Acad. Sci USA, 112(4), 1089-1094, doi: 10.1073/pnas.1415311112, 2015.

Marsh, R., Müller, S.A., Yool, A. and Edwards, N.R.: Incorporation of the C-GOLDSTEIN efficient climate model into the GENIE framework:“eb_go_gs” configurations of GENIE, Geosci. Model Dev., 4, 957-992, doi: 10.5194/gmd-4-957-2011, 2011.

McDonnell, A.M., Boyd, P.W. and Buesseler, K.O.: Effects of sinking velocities and microbial respiration rates on the attenuation of particulate carbon fluxes through the mesopelagic zone. Global Biogeochem. Cy., 29(2), 175-193, doi: 10.1002/2014GB004935, 2015.

Meyer, K.M., Ridgwell, A. and Payne, J.L.: The influence of the biological pump on ocean chemistry: implications for long-term trends in marine redox chemistry, the global carbon cycle, and marine animal ecosystems, Geobiology, 14(3), 207-219, doi: 10.1111/gbi.12176, 2016.

Maier-Reimer, E.: Geochemical cycles in an ocean general circulation model. Preindustrial tracer distributions, Global Biogeochem. Cy., 7(3), 645-677, doi: 10.1029/93GB01355, 1993.

Monteiro, F.M., Pancost, R.D., Ridgwell, A. and Donnadieu, Y.: Nutrients as the dominant control on the spread of anoxia and euxinia across the Cenomanian-Turonian oceanic anoxic event (OAE2): Model-data comparison, Paleoceanography, 27(4), doi: 10.1029/2012PA002351, 2012.

Moore, J.K., Doney, S.C., Kleypas, J.A., Glover, D.M. and Fung, I.Y.:. An intermediate complexity marine ecosystem model for the global domain. Deep-sea res. Pt. II, 49(1-3), 403-462, doi: 10.1016/S0967-0645(01)00108-4, 2002.

Mouw, C.B., Barnett, A., McKinley, G.A., Gloege, L. and Pilcher, D.: Global ocean particulate organic carbon flux merged with satellite parameters, Earth Syst. Sci. Data., 8(2), 531, doi: 10.5194/essd-8-531-2016, 2016a.

Mouw, C.B., Barnett, A., McKinley, G.A., Gloege, L. and Pilcher, D.: Phytoplankton size impact on export flux in the global ocean. Global Biogeochem. Cy., 30(10), 1542-1562, doi: 10.1002/2015GB005355, 2016b.

Najjar, R.G., Jin, X., Louanchi, F., Aumont, O., Caldeira, K., Doney, S.C., Dutay, J.C., Follows, M., Gruber, N., Joos, F. and Lindsay, K.: Impact of circulation on export production, dissolved organic matter, and dissolved oxygen in the ocean: Results from Phase II of the Ocean Carbon-cycle Model Intercomparison Project (OCMIP-2), Global Biogeochem. Cycles, 21(3), GB3007, doi:10.1029/2006GB002857, 2007.

Parekh, P., Follows, M.J. and Boyle, E.A.: Decoupling of iron and phosphate in the global ocean, Global Biogeochem. Cy., 19(2), doi: 10.1029/2004GB002280, 2005.

Paul, C., Matthiessen, B. and Sommer, U.: Warming, but not enhanced CO2 concentration, quantitatively and qualitatively affects phytoplankton biomass, Mar. Ecol. Prog. Ser., 528, 39-51, doi: 10.3354/meps11264, 2015.

Pörtner, H.O., Karl, D.M., Boyd, P.W., Cheung, W., Lluch-Cota, S.E., Nojiri, Y., Schmidt, D.N., Zavialov, P.O., Alheit, J., Aristegui, J. and Armstrong, C.: Ocean systems. In Climate change 2014: impacts, adaptation, and vulnerability. Part A: global and sectoral aspects. contribution of working group II to the fifth assessment report of the intergovernmental panel on climate change (pp. 411-484). Cambridge University Press. 2014.

Redfield, A.C., 1963. The influence of organisms on the composition of seawater. The Sea, 2, 26-77.

Reusch, T.B. and Boyd, P.W.: Experimental evolution meets marine phytoplankton, Evolution, 67(7), 1849-1859, doi: 10.1111/evo.12035, 2013.

Ridgwell, A.J.: Glacial-interglacial perturbations in the global carbon cycle, PhD Thesis University of East Anglia Norwich. 2001.

Ridgwell, A., Hargreaves, J.C., Edwards, N.R., Annan, J.D., Lenton, T.M., Marsh, R., Yool, A. and Watson, A.: Marine geochemical data assimilation in an efficient Earth System Model of global biogeochemical cycling, Biogeosciences, 4(1), 87-104, doi: 10.5194/bg-4-87-2007, 2007.

Ridgwell, A. and Schmidt, D.N.: Past constraints on the vulnerability of marine calcifiers to massive carbon dioxide release, Nat. Geosci., 3(3), p.196. doi: 10.1038/ngeo755, 2010.

Rosengard, S.Z., Lam, P.J., Balch, W.M., Auro, M.E., Pike, S., Drapeau, D. and Bowler, B.: Carbon export and transfer to depth across the Southern Ocean Great Calcite Belt. Biogeosciences, 12(13), 3953-3971, doi: 10.5194/bg-12-3953-2015, 2015.

Rubino, M., Etheridge, D.M., Trudinger, C.M., Allison, C.E., Battle, M.O., Langenfelds, R.L., Steele, L.P., Curran, M., Bender, M., White, J.W.C. and Jenk, T.M.: A revised 1000 year atmospheric δ13C-CO2 record from Law Dome and South Pole, Antarctica. J. Geophys. Res-Atmos., 118(15), 8482-8499, doi: 10.1002/jgrd.50668, 2013.

Sarmiento, J.L.J.L., Gruber, N.N.: Ocean Biogeochemical Dynamics, 1015 Princeton University Press Princeton, 2006.

Schmittner, A., Gruber, N., Mix, A.C., Key, R.M., Tagliabue, A. and Westberry, T.K.: Biology and air–sea gas exchange controls on the distribution of carbon isotope ratios (δ 13 C) in the ocean, Biogeosciences, 10(9), 5793-5816, doi: 10.5194/bg-10-5793-2013, 2013.

Segschneider, J. and Bendtsen, J.: Temperature-dependent remineralization in a warming ocean increases surface pCO2 through changes in marine ecosystem composition. Global Biogeochem. Cy., 27(4), 1214-1225, doi: 10.1002/2013GB004684, 2013.

Steinberg, D.K. and Landry, M.R.: Zooplankton and the ocean carbon cycle, Annu. Rev. Mar. Sci., 9, 413-444, doi: 10.1146/annurev-marine-010814-015924, 2017.

Taucher, J. and Oschlies, A.: Can we predict the direction of marine primary production change under global warming?, Geophys. Res. Lett., 38(2), doi: 10.1029/2010GL045934, 2011.

Turner, J.T.: Zooplankton fecal pellets, marine snow, phytodetritus and the ocean's biological pump. Prog. Oceanogr., 130, 205-248, doi: 10.1016/j.pocean.2014.08.005, 2015.

U.S. DOE.: Carbon Cycling and Biosequestration: Report from the March 2008 Workshop, DOE/SC-108, U.S. Department of Energy Office of Science, 81, 2008.

Ward, B.A., Wilson, J.D., Death, R.M., Monteiro, F.M., Yool, A. and Ridgwell, A., 2018. EcoGEnIE 1.0: plankton ecology in the cGEnIE Earth system model. Geosci. Model Dev., 11(10), pp.4241-4267, doi: 10.5194/gmd-11-4241-2018, 2018.

Weber, T., Cram, J.A., Leung, S.W., DeVries, T. and Deutsch, C.: Deep ocean nutrients imply large latitudinal variation in particle transfer efficiency, P. Natl. Acad. Sci USA, 113 (31), 8606-9611, doi: 10.1073/pnas.1604414113, 2016.

Wilson, J.D., Barker, S. and Ridgwell, A.: Assessment of the spatial variability in particulate organic matter and mineral sinking fluxes in the ocean interior: Implications for the ballast hypothesis. Global Biogeochem. Cy., 26(4), doi: 10.1029/2012GB004398, 2012.

Yamamoto, A., Abe-Ouchi, A. and Yamanaka, Y.: Long-term response of oceanic carbon uptake to global warming via physical and biological pumps. Biogeosciences, 15(13), 4163-4180, doi: 10.5194/bg-15-4163-2018, 2018.

	Rate constant as T approaches infinity (*a*)	Multiplier constant for T (*1/b*)	Reference
~~A~~	~~1/b~~		
~~Eppley et al. 1972~~Eppley curve	0.59	0.0633	Eppley et al. 1972
~~Bissinger et al. 2008~~LPD curve	0.81	0.0631	Bissinger et al. 2008

Table 1, Values for variables in ~~eqn~~ Eq. 4~~2~~

Name	Circulation	Bio~~geo~~chemistry	1. Temperature-dependent uptake	2. Temperature-dependent remineralisation	Temperature-dependent~~ed~~ DOM production (both) and	Description
~~CB~~STND	✓ ~~☒~~	✓~~*~~				Standard model
~~CBRU~~TDEP	✓~~*~~	✓~~*~~	✓~~*~~	✓~~*~~		Temperature-dependent POM model
$TDEP_{+TDOM}$	✓	✓	✓	✓	✓	Temperature-dependent POM and DOM model

Table 2, Model settings, processes included in each set-up. Column numbering corresponds to numbering in figure 1.

~~Variable~~Parameter	Values applied
Vmax	4,7,10
POC fraction 2 (recalcitrant)	0.002, **0.008**, 0.032
Ea(1) (labile fraction) x10^3J/mol	53, 54, **55**, 56, 60

Table 3, settings for ~~variables~~ parameters in ~~CBRU~~TDEP (temperature-dependent). Values in bold are those ~~used~~ applied in John et al. 2014.

	Standard Deviation				CRMSD			correlation		
	Data	STND	TDEP	$TDEP_{+TDOM}$	STND	TDEP	$TDEP_{+TDOM}$	STND	TDEP	$TDEP_{+TDOM}$
Whole ocean PO_4	0.8072	0.8072	0.7386	0.7606	0.2208	0.2043	0.2113	0.9236	0.9227	0.9177
Surface PO_4	0.6026	0.5009	0.4452	0.3921	0.1699	0.1820	0.2130	0.9350	0.9294	0.9274
Whole ocean O_2	1.6461	1.5154	1.3900	1.4522	0.5476	0.5501	0.5356	0.8670	0.8615	0.8703
O_2 283m to 411m	1.7285	1.3724	1.6531	1.6142	0.8145	0.8443	0.8200	0.7551	0.7660	0.7746

Table 4, Statistics for the fit of the model to phosphate and oxygen distribution in the present day for the STND, TDEP (best-fit) and $TDEP_{+TDOM}$ simulations. Statistics shown as standard deviation (SD) in µmol/l, centred root mean square difference (CRMSD) in µmol/l, and correlation to data. $TDEP_{+TDOM}$ is described in section 5.2.

	DOM production ratio	surface DOM lifetime (yr)	Surface DOM concentration (mol/kg)
STND	0.6600	0.5000	11.5×10^{-6}
TDEP	0.6600	0.5000	17.7×10^{-6}
$TDEP_{+DOMtprod}$	0.6685	0.5000	20.3×10^{-6}
$TDEP_{+DOMtremin}$	0.6600	0.4753	13.9×10^{-6}
$TDEP_{+TDOM}$	0.6677	0.4907	13.4×10^{-6}

Table 5, Present (2010) DOM parameters.

	DOM production ratio change (%)	surface DOM lifetime change (%)	Surface DOM concentration change (%)
STND	0.00	0.00	-2.07
TDEP	0.00	0.00	0.54
$TDEP_{+DOMtprod}$	0.99	0.00	2.89
$TDEP_{+DOMtremin}$	0.00	-4.38	-2.52
$TDEP_{+TDOM}$	-0.33	-0.75	-0.74

Table 6, Anomaly (as %) DOM parameters for 2010 with respect to 1700.

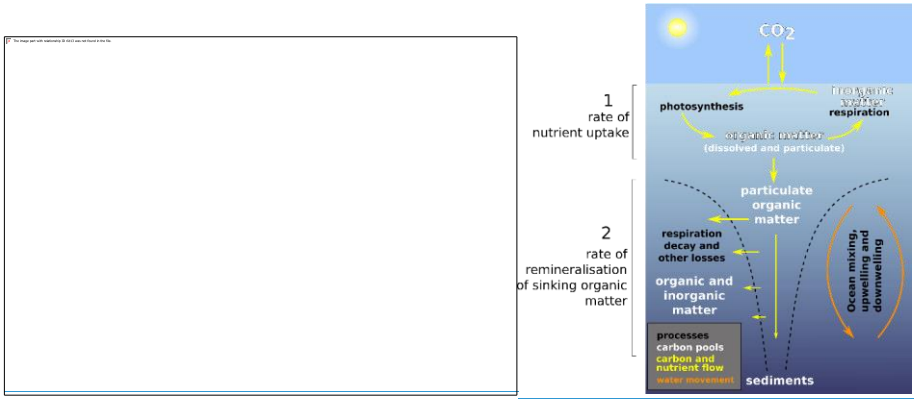

Figure 1, Simplified schematic of the ocean biological pump and dissolved nutrient movements, and the two temperature-dependent processes that are considered in this study 1. Nutrient uptake rates, 2. Remineralisation rate. In the style of U.S. DOE (2008). We do not model sediments in this study, but it appears in the figure for completeness.

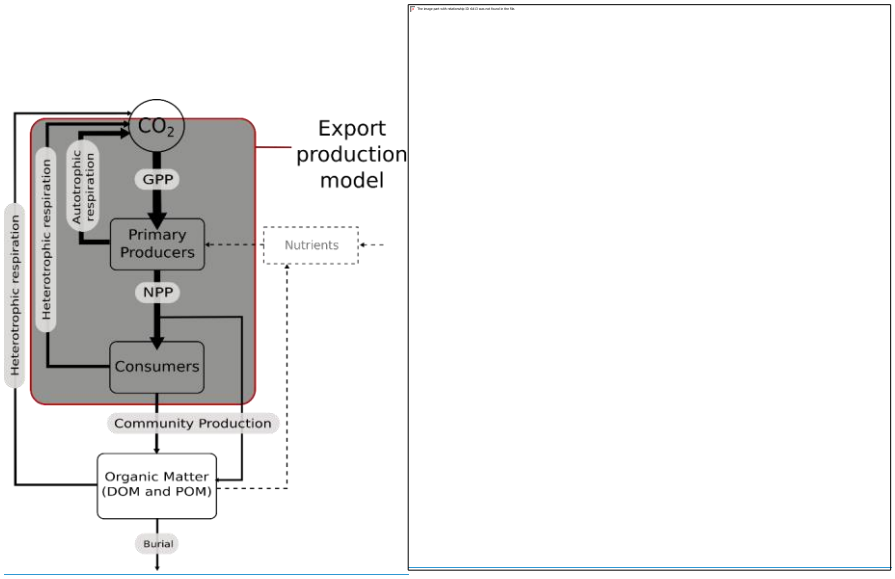

Figure 2. Schematic of biological pump processes showing where cGENIEs export production operates. **In the export production model, no mechanistic consideration of** the effects of temperature within the **mixed** ~~p~~**layer** (i.e. GPP vs NPP vs community production) ~~plankton respiration vs photosynthesis (GPP) temperature dependence~~ **can be considered, but** ~~microbial~~ heterotrophic **respiration** (as remineralisation) **vs community production** (as export production) **can be considered, as well as nutrient recycling** ~~nearer the surface~~**.** In this study we apply temperature dependency to Organic Matter production and remineralisation that drives the biological carbon pump. We do not model burial in this version of cGENIE (but it is here for completeness). In this cGENIE configuration, the nutrient is phosphate. Dashed line indicates the cycling (and re-supply due to circulation) of nutrients. Solid lines indicates the cycling of carbon.

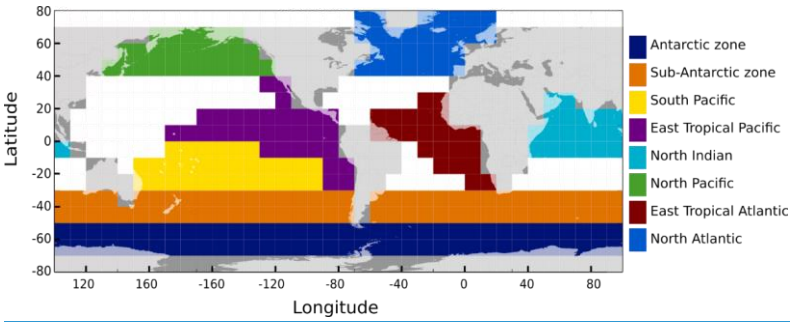

Figure 3, Selected ocean regions for model-data comparison (on a 10x10 degree grid, with land masses overlaid for indication), based on Weber et al. (2016) and WOA 2009 data (Levitus et al., 2010)**.**

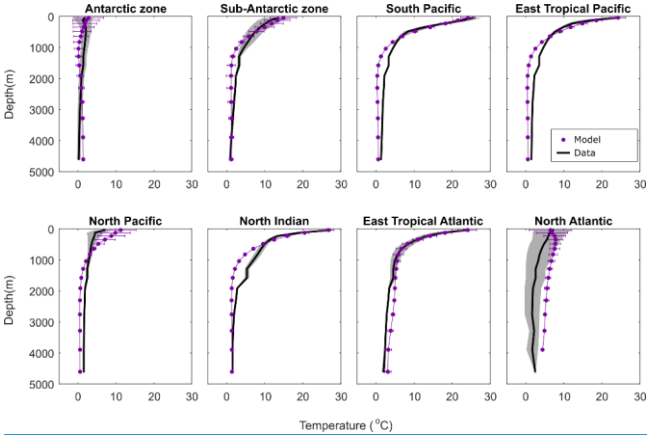

Figure 4, Temperature (°C) per depth by region for model and data (mean and standard deviation). Data from WOA 2009 (Levitus et al., 2010).

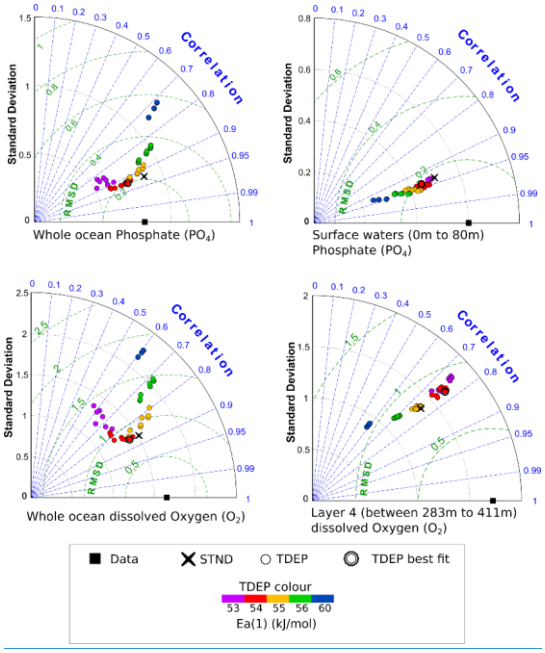

Figure 5, Taylor diagrams for model fit to data for PO_4 and O_2 concentrations, showing standard deviation (standard deviation is not normalised), correlation and root means squared ~~error~~ difference (RMSD). Data from WOA 2009 (Levitus et al., 2010). The best fit TDEP setting is double circled.

875

Formatted: Subscript

Formatted: Subscript

Formatted: Normal

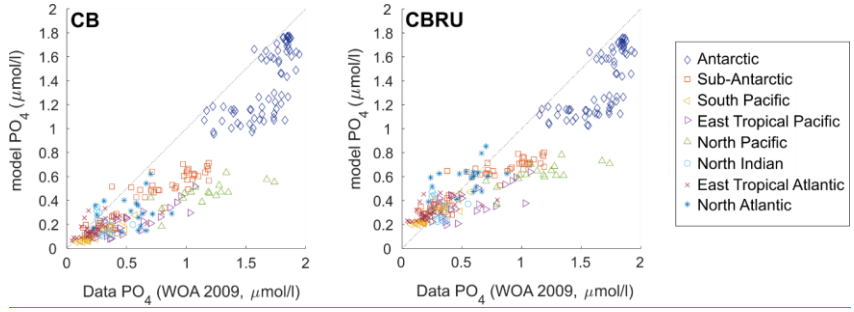

Figure 6, Cross plot for surface (0m to 80m) PO_4 concentrations (µmol l^{-1}) for data and model labelled by ocean region. Data from WOA 2009 (Levitus et al., 2010)

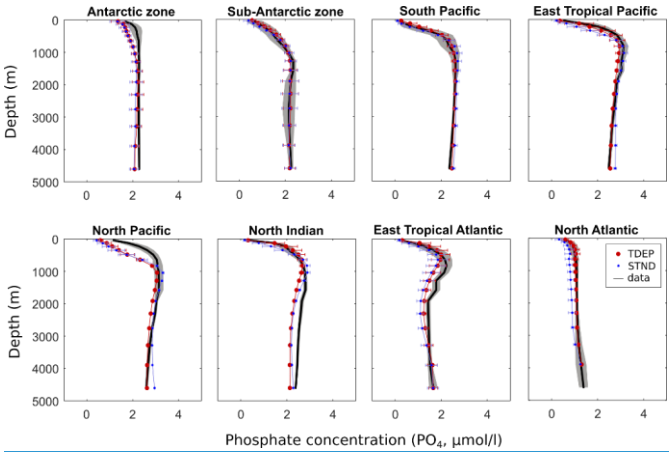

Figure 7, PO_4 (µmol l^{-1}) per depth by region for model and data (mean and standard deviation). Data from WOA 2009 (Levitus et al., 2010). ~~CB~~STND is standard model, ~~CBRU~~TDEP is temperature- dependent model.

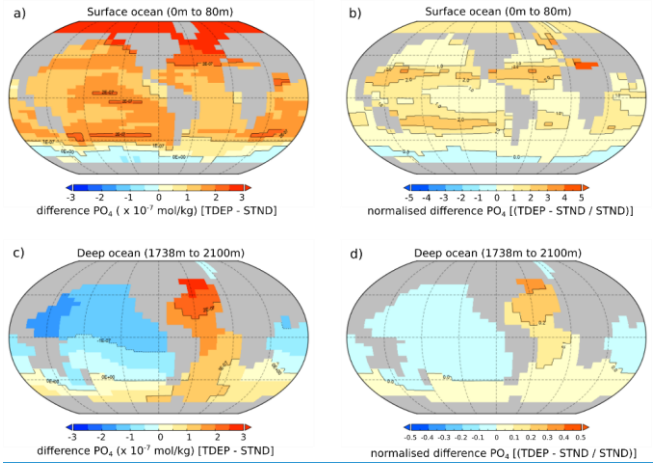

Figure 8, DNormalised difference in PO_4 concentration in best-fit CBRUTDEP compared to CBSTND, a) and b) surface waters (0m to 80m), c) and d) deep waters 1738m to 2100m). Left a) and c) absolute difference (mol/kg), right b) and d) normalised difference. (bothAll are the present-day, note scale difference on normalised difference between surface and deep). CBSTND is standard model, CBRUTDEP is temperature dependent model.

Formatted: Normal

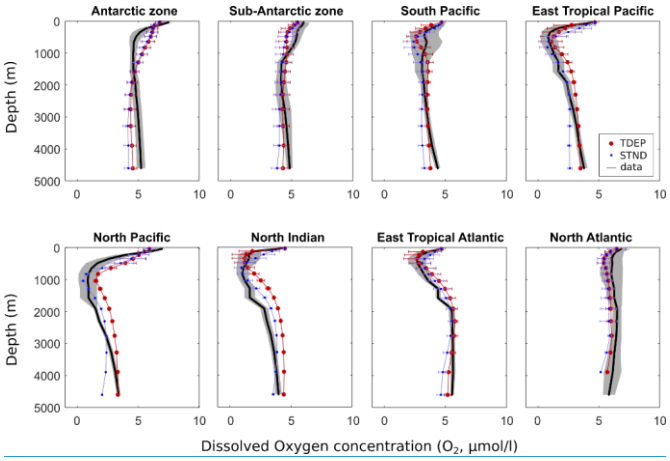

Figure 9, Dissolved O_2 (µmol l^{-1}) per depth by region for model and data (mean and standard deviation). Data from WOA 2009 (Levitus et al., 2010). ~~CB~~STND is standard model, ~~CBRU~~TDEP is temperature-dependent model.

Formatted: Normal

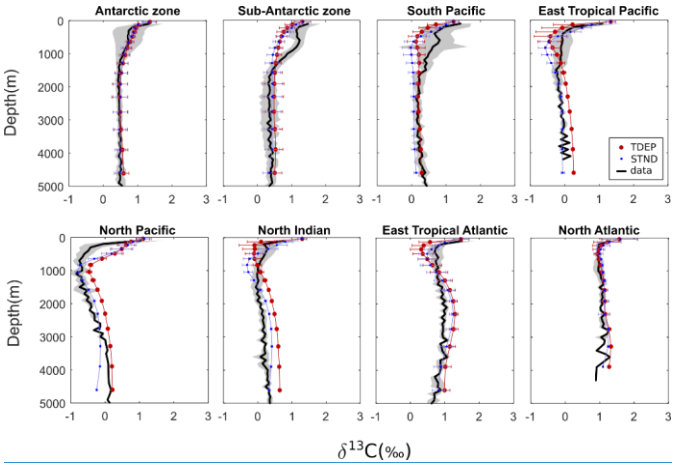

Figure 10, $\delta^{13}C$ of DIC (‰ VPDB) per depth by region for model and data (mean and standard deviation). Data from Schmittner et al. (2013). ~~CB~~STND is standard model, ~~CBRU~~TDEP is temperature~~-~~dependent model.

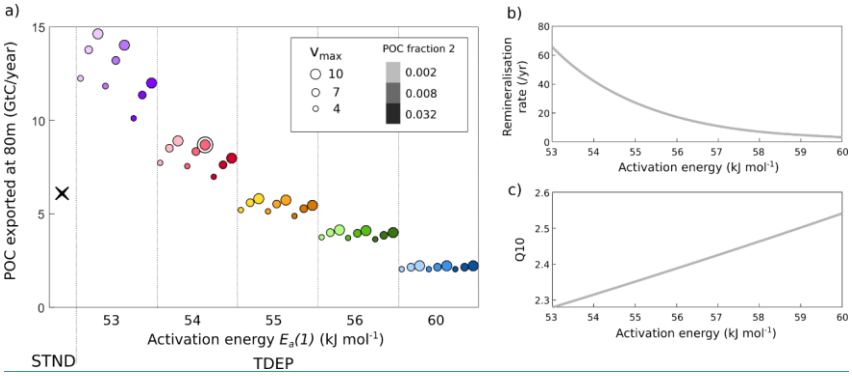

Figure 11, Global POC flux (GtC yr^{-1}) at 80m (a) and the effect of activation energy on (b) remineralisation rate and (c) Q10 (for a 0°C to 10°C change). In a) ~~Standard~~STND model is shown as a black cross, ~~Temperature-dependent~~TDEP model are circles. Best fit ~~CBRU~~TDEP setting is double circled. ~~CB~~STND is standard model, ~~CBRU~~TDEP is temperature-dependent model. Colours in a) reflect those used in figure 5.

Formatted: Normal

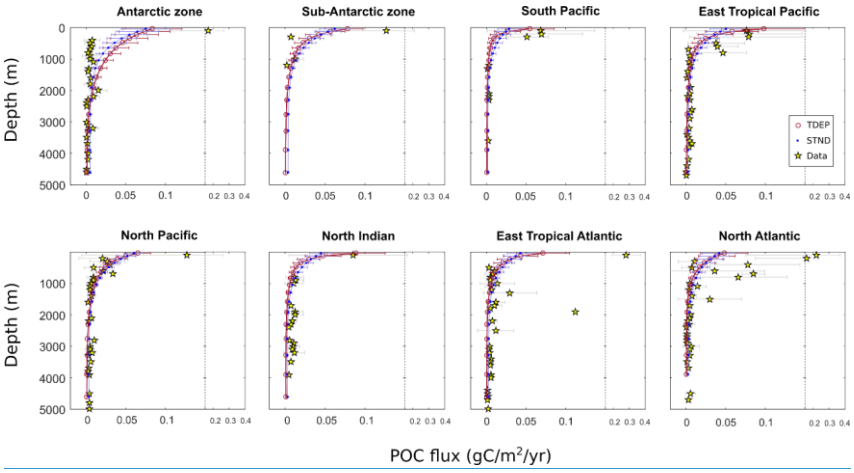

910 **Figure 12, POC flux (gC m^{-2} yr^{-1}) for model (mean and standard deviation) and data. Data from Mouw et al., (2016a). ~~CB~~STND is standard model, ~~CBRU~~TDEP is temperature-dependent model.**

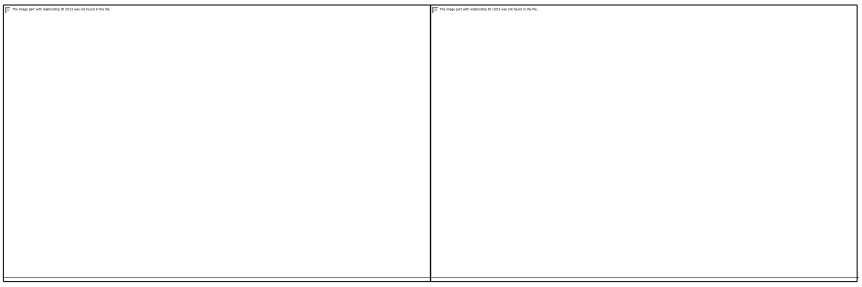

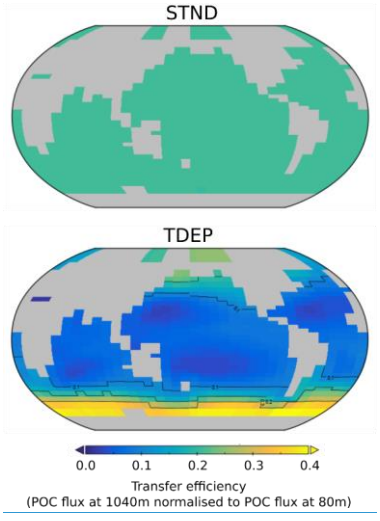

Figure 13, Model POC transfer efficiency (also ~~here~~ used as a measure of biological carbon pump efficiency here) for ~~C~~BSTND (~~left~~top) and best fit ~~CBRU~~TDEP (~~right~~bottom). Transfer efficiency is the fraction of POC exported at 80m that reaches 1040m, for the year 2010. Global transfer efficiency value for STND is 0.208.

Formatted: Normal

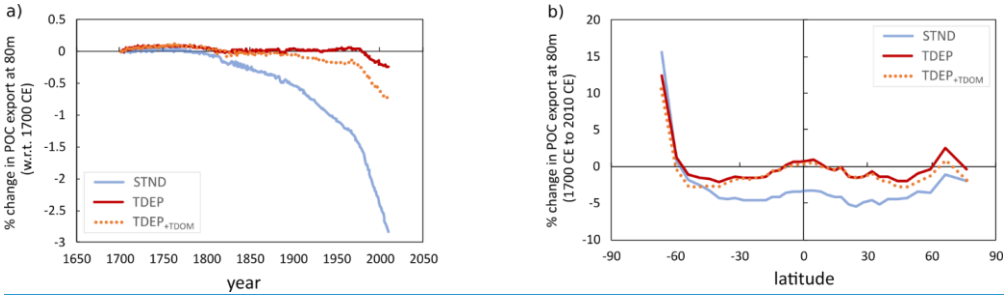

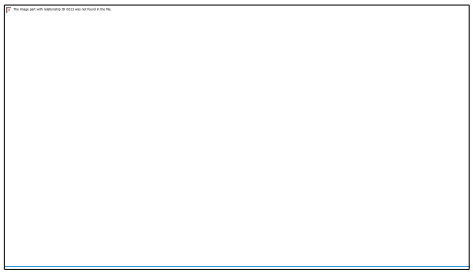

Figure 14, POC export at 80m, % change with respect to (w.r.t) the year 1700, a) global mean POC export at 80m, b) latitudinal mean POC export change at 2100 w.r.t. 1700CE. ~~CB~~STND is standard model, ~~CBRU~~TDEP is temperature- dependent model, $TDEP_{+TDOM}$ is temperature-dependent POM and is described in section 5.2.

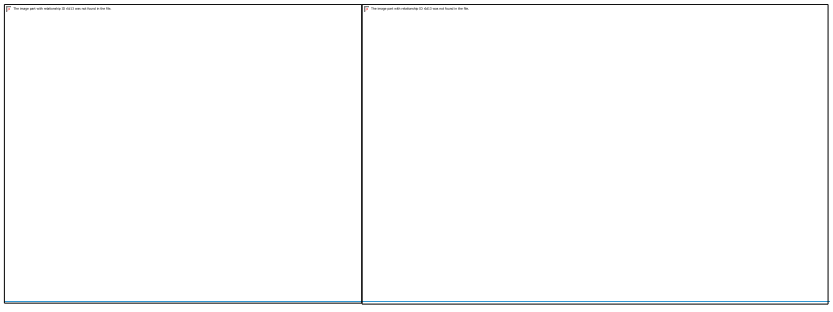

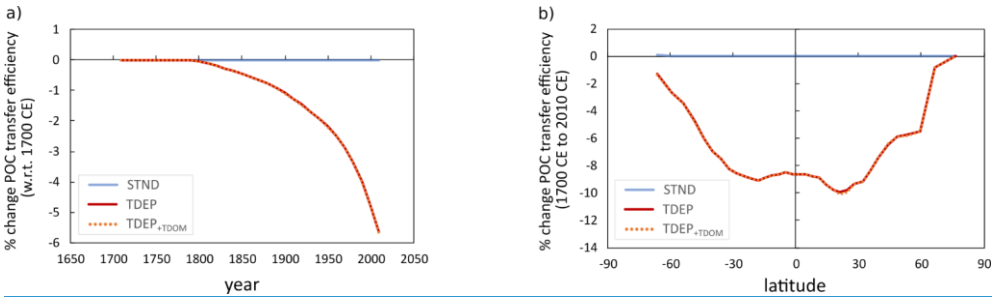

Figure 15, TDEP bBiological pump "transfer efficiency" (the proportion of POC exported at 80m that reaches 1040m) % change with respect to 1700 CE., a) Gglobal mean change per year (left) w.r.t 1700; b) latitudinal change at the year 2010 w.r.t 1700 (right). CBRUSTND is standard model, TDEP is temperature- dependent model, TDEP+TDOM is temperature-dependent POM and DOM and ,is described in section 5.2.

Formatted: Normal

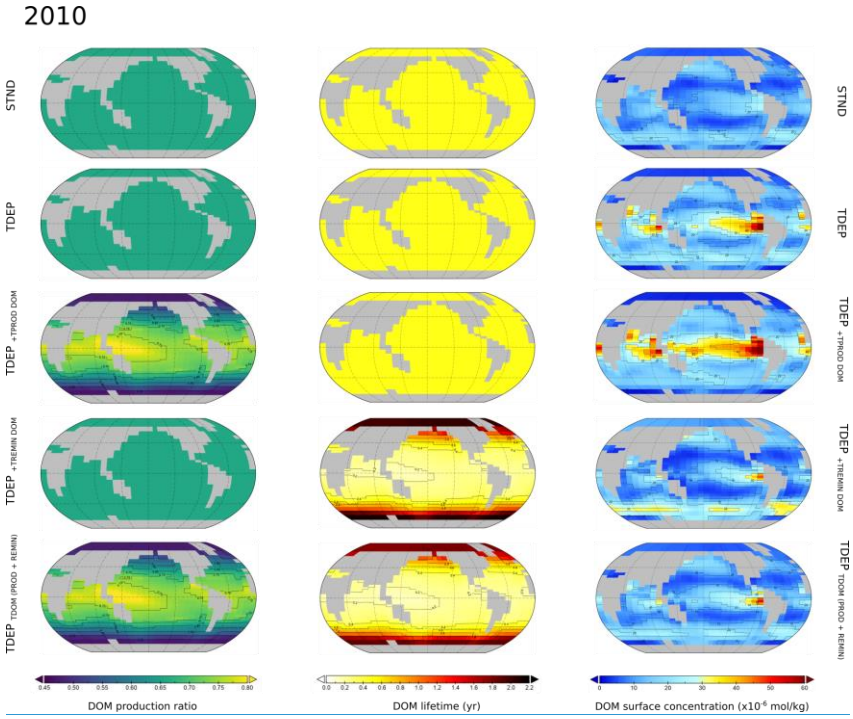

Figure A1, Surface ocean DOM production ration, DOM lifetime and DOM concentration for the modelled present day (year 2010). Labelled simulations include those discussed in the main text (STND, TDEP and $TDEP_{e\text{-}TDOM}$), $TDEP_{e\text{-}TDOM}$ labelled here as $TDEP_{TDOM(PROD+REMIN)}$ for clarity. Also mapped is DOM production and remineralisation temperature dependence separately applied as $TDEP_{e\text{-}TPROD\ DOM}$, $TDEP_{e\text{-}TREMIN\ DOM}$).

Formatted: Subscript
Formatted: Subscript
Formatted: Subscript
Formatted: Subscript
Formatted: Subscript
Formatted: Subscript
Formatted: Subscript

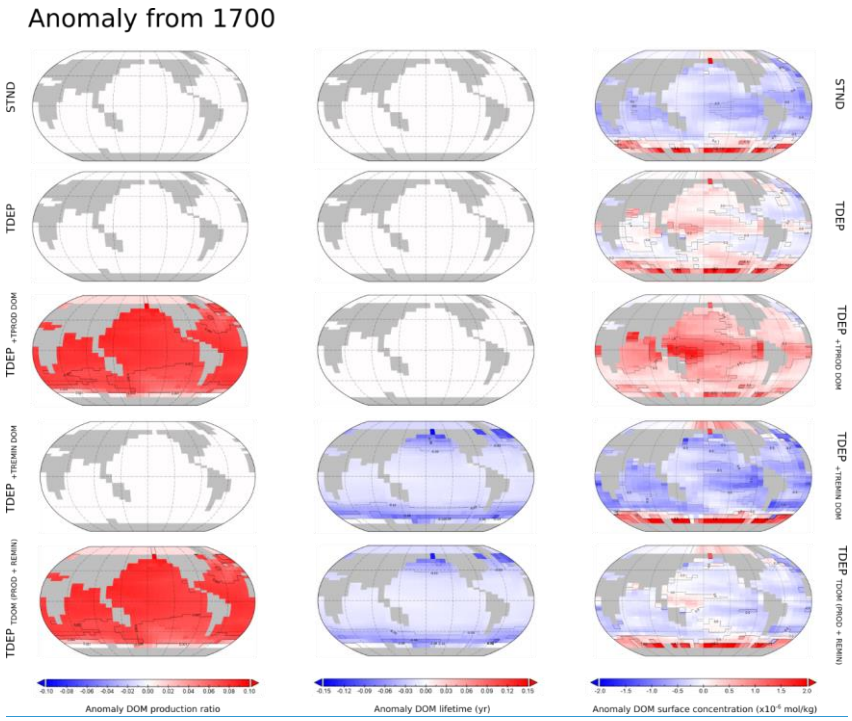

Figure A2, Anomalies for the present day against the year 1700 for surface ocean DOM production ratio, DOM lifetime and DOM concentration for the modelled present day. Labelled simulations include those discussed in the main text (STND, TDEP and $TDEP_{\epsilon TDOM}$), $TDEP_{\epsilon TDOM}$ labelled here as $TDEP_{TDOM(PROD+REMIN)}$ for clarity. Also mapped is DOM production and remineralisation temperature dependence separately applied as $TDEP_{+TPROD\ DOM}$ $TDEP_{+TREMIN\ DOM}$).

Formatted: Normal

Formatted: Subscript

Formatted: Subscript